[American Journal of Science, Vol. 311, September, 2011, P. 573–607, DOI 10.2475/07.2011.01]

American Journal of Science

SEPTEMBER 2011

SELF-ACCELERATING DOLOMITE-FOR-CALCITE REPLACEMENT: SELF-ORGANIZED DYNAMICS OF BURIAL DOLOMITIZATION AND ASSOCIATED MINERALIZATION

ENRIQUE MERINO* and ÀNGELS CANALS**

ABSTRACT. A new dynamic model of dolomitization predicts a multitude of textural, paragenetic, geochemical and other properties of burial dolomites. The model is based on two postulates, (1) that the dolomitizing brine is Mg-rich but *under*saturated with both calcite and dolomite, and (2) that the dolomite-for-calcite replacement happens not by dissolution-precipitation as usually assumed, but by dolomite-growth-driven pressure solution of the calcite host. Crucially, the dolomite-for-calcite replacement turns out to be self-accelerating *via* Ca^{2+}: the Ca^{2+} released by each replacement increment accelerates the rate of the next, and so on. As a result, both pore-fluid Ca^{2+} and replacement rate grow exponentially.

As brine enters and infiltrates a limestone, water/rock disequilibrium plus the self-accelerating feedback inevitably yield a process that is self-organized, both in time (as repeated dolomite growth pulses per slice of limestone) and in space (as successive slices). Self-organization in pulses and slices accounts for several properties of burial dolomites: (1) generation of dissolution porosity and its spatially periodic distribution; (2) dolomitization affects only limestones; (3) sharp field contacts between dolomitized and undolomitized limestone; (4) formation of both saddle dolomite and "late-stage" calcite near the end of each growth pulse, accompanied by Mississippi-Valley-type ores if the brine also contains Zn, Pb, Ba, sulfate, and other relevant elements; (5) "sweeping" of ores downflow with accumulation in the last position of the dolomitization front.

In addition, the combination of the self-accelerating feedback *via* Ca^{2+} with the known strain-rate-softening rheology of crystalline carbonates leads to another suite of predictions that are strikingly confirmed by observation. If the dolomite-for-calcite replacement becomes fast enough to lower the local rock viscosity sufficiently, then the dolomite growth will pass spontaneously from replacive to displacive. This is when thin, self-organized, displacive zebra veins form (Merino and others, 2006), indeed displaying *seamless* contacts with their replacive walls and consisting of *curved*, or saddle, dolomite crystals. Serendipitously, both the deformation of the dolomite crystals (produced by Ca-for-Mg substitution driven by the huge pore-fluid Ca^{2+}) and the seamless rheological transition result from the self-accelerating feedback *via* Ca^{2+} itself; that is why they are always associated. This detail alone strongly suggests that the new model captures the chemistry, drives, mechanisms, and feedbacks that lend burial dolomitization and its often associated MVT ore deposits their geological uniqueness.

Key words: Dolomitization dynamics, chemical-rheological feedbacks, self-organization, replacement physics, petrography of replacement, geochemistry's blind spot, dolostone porosity, dolomitizing brines, replacive-to-displacive dolomite transition, syntaxial zebra veins, MVT lead-zinc ores, saddle dolomite, late-stage calcite, dedolomitization

* Department of Geological Sciences, Indiana University, 1001 East 10th Street, Bloomington, Indiana 47405, USA; merino@indiana.edu

** Departament de Cristal.lografia, Mineralogia i Dipòsits Minerals, Facultat de Geologia, Universitat de Barcelona, Martí i Franquès s/n, 08028 Barcelona, Spain; angelscanals@ub.edu

I. INTRODUCTION

Huge volumes of limestone have been transformed into dolostone by replacement of calcite by dolomite in many ancient sedimentary basins. Although the transformation may seem chemically simple—just add Mg to calcite to make dolomite— and despite extensive research by petrologists and geochemists for decades, several aspects of the metasomatic process of dolomitization and several properties of burial dolomites are poorly understood: Why are *only* limestones dolomitized, and not other rocks? What causes the large porosity that makes burial dolostones excellent petroleum reservoirs? What are the source, nature, and chemistry of the dolomitizing aqueous solutions? How do those Mg-rich brines travel to the site of dolomitization? Is burial dolomitization fast or slow? What are the mechanisms of formation of the two basic types of dolomite, the replacive and the zebra/breccia veins (which are displacive), and why are they associated? Why are the zebra veins thin and equidistant, have no sharp contact with their walls, and consist of dolomite crystals that are curved (thus called saddle dolomite), displaying a consistent assemblage of enigmatic textures? Why is dolomitization of limestones paradoxically accompanied by formation of so-called late-stage calcite and even dedolomitization, or calcite-for-dolomite replacement? Why are the distinctive Mississippi-Valley-type (MVT) ore deposits—consisting of barite, fluorite, sphalerite, galena, and other minerals—typically hosted in burial dolomites? The prevailing theory of dolomitization, gives only *ad hoc* or unsatisfactory answers to those questions. Furthermore, it contains a flaw that we believe is both fundamental and hidden from view: Whereas according to the prevailing theory replacement, and in particular the dolomite-for-calcite replacement, is produced by "dissolution-precipitation," alert early investigators (Bastin and others, 1931) long ago showed petrographically that replacement *cannot* be produced by dissolution-precipitation. Thus, in the section "Replacement Physics" we discuss the evidence against dissolution-precipitation, why both the old petrographic insights and their kinetic implications were forgotten, and how replacement does take place, in light of recent theoretical rheological-kinetic research.

The main purpose of this paper is to propose a new view of dolomitization dynamics that may solve many of the problems of prevailing dolomitization theories; several of these problems are summarized in Section II. The new model is a forward model, one based on two postulates. The first arises in contrast to the widespread assumption that the dolomitizing brine must be supersaturated with dolomite. If so, any rock type could in principle be dolomitized, whereas in fact only limestones are. Therefore, in the new model we assume that the dolomitizing aqueous solution must be Mg-rich but—counterintuitively—*under*saturated with dolomite and with calcite.

The second postulate is that replacement, and in particular the dolomite-for-calcite replacement, takes place not by dissolution-precipitation, but by guest-growth-driven *pressure solution* of the host. This mechanism—as significant for weathering, diagenesis, ore genesis, and metamorphism as it is for dolomitization—is justified in Section III (Replacement Physics).

In the main section of this paper, Section IV, "New Dolomitization Model," we describe how the two postulates of the model, combined with kinetic and rheological feedbacks inevitable in the transformation of limestone into dolostone, lead to predicting a complex, non-linear, self-organized dolomitization process that yields the two observed dolomite types (replacive and displacive, or dolomite-I and dolomite-II) characteristic of burial dolostones along with a multitude of textural, paragenetic, geological, geochemical, rheological, dynamic, and field properties. All the predictions are confirmed by independent evidence, suggesting the new model is on the right path. Although the new model is conceptual, some of its mechanisms (in particular the self-accelerating kinetics of the dolomite-for-calcite replacement) are

quantified in two Appendices. Implications of the new dynamics are discussed in Section V, including its use as a framework for future reaction-transport calculations of dolomitization and associated mineralization. A Summary of the new paradigm is given in the last section, Section VI.

II. WEAKNESSES OF THE PREVAILING THEORY OF BURIAL DOLOMITIZATION

According to the consensus reached in recent decades (for example, Zenger and Dunham, 1980; Land, 1980; Yao and Demicco, 1997; Nielsen and others, 1998; Gregg and others, 2001; Wilkinson, 2003; Gregg, 2004; Machel, 2004; Gasparrini and others, 2006; Lonee and Machel, 2006; Davies and Smith, 2006) burial dolomitization is thought to take place in two stages separated in time. In the first stage, a huge volume of limestone is replaced by dolomite—the so-called dolomite-I, or replacive dolomite—via dissolution-precipitation driven by a Mg-rich, dolomite-supersaturated brine, possibly evaporative, which in some versions of the theory comes down from the surface environment. An example of replacive dolomite, or dolomite-I, is shown in figure 1A. The replacive dolostone is then assumed to undergo a void-opening process—by fracturing, hydraulic fracturing, karst dissolution, or hydrothermal alteration—and eventually a second phase of dolomite, the so-called dolomite-II, or "void-filling cement," grows in those voids from a new, hot brine also supposedly supersaturated with dolomite. This dolomite-II often occurs as sets of zebra and "breccia"-like veins (figs. 1B, 1C, 1D, and 1E), textures that are common also in Mississippi-Valley-type (MVT) ore-deposits.

There are several problems with the consensus model.

(1) It takes for granted that two phases of dolomite growth (thought to have formed from different brines), the hypothetical void-opening process between them, and MVT ore growth (often hosted in these dolostones) must all coincide in space and in the appropriate temporal sequence, in most burial dolostones.

(2) As noted, if the dolomitizing brine is assumed to be supersaturated with dolomite from the start *any* rock type could in principle be dolomitized. In fact only limestones can be dolomitized. Furthermore, for some investigators the assumption points to seawater, supersaturated with respect to dolomite, as a candidate for the dolomitizing brine. This choice leads to predicting a dolomitization effected by descending, low-temperature solutions (unless one calls for dolomitization by convecting sea-water, for example Machel, 2004). Each of the two implications is contradicted by good evidence. Gasparrini and others (2006) show large ascending fingers of dolomitization into Paleozoic limestones in NW Spain, see figures 2A, 2B; and fluid inclusion data published by many geochemists leave little doubt that dolomitization (dolomite I and dolomite II) happens between 70 and 200 °C, which means dolomitization by solutions that are hot.

(3) The prevailing view sheds no light on the origin of the remarkable assemblage of textures systematically displayed by dolomite-II or on its association with dolomite-I. Dolomite-II occurs as thin, white, zebra and breccia-like veins displaying seamless contacts with the replacive dolomite-I of the walls and consisting of coarse saddle-shaped crystals; see figures 1B to 1E. First, if the two dolomites are supposed to be independent and separated in time, why is their contact always gradual, seamless, and optically continuous, instead of sharp under the microscope, as one would expect? Second, while the zebra veins and breccia veins are routinely referred to in the literature as "void-filling cement," we presented evidence (Merino and others, 2006) indicating that the dolomite-II veins are not cements, but displacive veins. The evidence includes: (a) small transform-fault displacements of veins that could not have taken place if the veins were passive cements; (b) tiny stylolites in the slices of host dolomite-I that formed as the veins grew in order to compensate for the volume added by the veins. And (c), we showed theoretically that the same vein-growth-generated

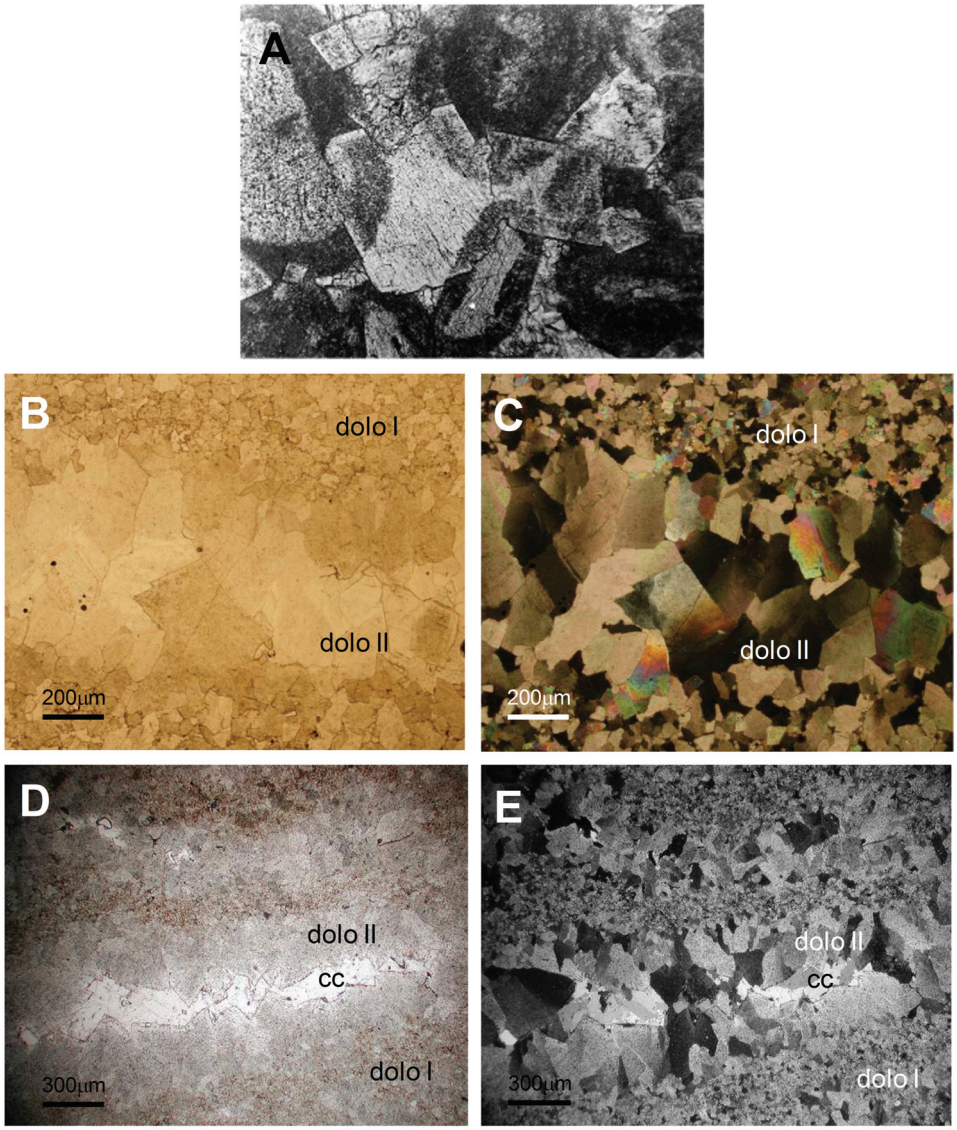

Fig. 1. Textural properties of replacive and displacive dolomite in burial dolomitization. (A) A dolomite rhombohedron 0.8 mm across replaces parts of three oolites at once. The facts that the dolomite crystal is idiomorphic and that the replacement preserves the oolitic rings undeformed (and thus preserves mineral volume) each separately rules out that it was produced by dissolution-precipitation; see text. (1960 photomicrograph reproduced with permission from its author, Raymond C. Murray.) (B, C) Plane-polarized and cross-polars views under low magnification of one zebra vein consisting of displacive dolomite (or dolomite-II), from the Cretaceous Basque-Cantabrian basin, northern Spain. In (B) note lack of sharp contact between the dolomite II vein (coarse crystalline) and its dolomite I walls (fine crystalline). In (C) note the sweeping extinction, denoting deformation of the structure, of several large saddle dolomite-II crystals. A few of these can be seen to grow in optical continuity with small crystals of dolomite-I; this is visible only while rotating the microscope stage and under higher magnification. (D, E) Plane-polarized and cross-polars views of displacive zebra veins of saddle dolomite in burial dolomites of SW Sardinia. Note the seamless contact between dolomite-I and dolomite-II, and the thin colorless late-stage calcite cement (cc) at center, with low optical relief. In (E) a few instances of saddle dolomite-II crystals in optical continuity with small crystals of dolomite-I are detectable under higher magnification while rotating the stage.

Fig. 2. Two views of the sharp contacts between ascending fingers of completely dolomitized (dark gray) and undolomitized Upper Carboniferous limestone (light gray), in the Southwestern Cantabrian Zone, NW Spain (Gasparrini and others, 2006). That the dolomitization *rose* through the limestone is particularly clear in (A), a photo by M. Gasparrini. (B), photo by À. Canals.

stress, or induced stress, that forcibly displaces the host also triggers a feedback that tends to pressure-dissolve, and thus "weed out," incipient veins that happen to be too close to their neighbors, leaving the surviving veins more equidistant than before, and explaining the self-organized nature of zebra veins that had been noted by Merino (1984) and Fontboté (1993). Third, the prevailing dolomitization theory also leaves

unexplained the facts that the veins are thin and bilateral and consist of crystals of dolomite that are curved and optically continuous with the replacive dolomite-I crystals of the walls.

(4) The prevailing theory leaves unclear what the *local* reactions of dolomitization really are. On the basis of oilfield-brine compositions from Oklahoma, Weyl (1960) demonstrated that dolomitization happens according to what he called an "approximate mass balance," 2calcite + Mg^{2+} = dolomite + Ca^{2+}, a mass balance involving calcite dissolution and dolomite precipitation, with carbonate being conserved between the two minerals over some mesoscopic scale left unspecified by Weyl. However, despite the fact that the mass balance does not apply to the *local,* subgrain scale, most investigators since Weyl (1960) have adopted it as the local reaction that brings about dolomitization, disregarding long-known petrographic evidence (see example in figure 1A discussed in the next section) showing that the local replacement does preserve mineral volume and should therefore be 1.74 calcite + Mg^{2+} + 0.26CO_3^{2-} = dolomite + 0.74Ca^{2+}, where the 1.74 factor approximately equals the dolomite formula volume, 64.3 cm^3, divided by the calcite formula volume, 36.9 cm^3. Also, use by recent modelers (Wilson and others, 2001; Jones and Xiao, 2005) of Weyl's mesoscopic mass balance in the continuity equation does not appear to meet the requirement that the reactions whose rates R_i are inserted in its reaction term must be *local*—that is, they must take place *within* a volume element small enough that the difference in J_i flux across it, between entry and exit, can be approximated as linear; only then can quadratic and higher-order terms (in the width of the volume element) in a Taylor expansion of the flux be neglected. (See the derivation of the mass conservation equation in Robinson and Stokes, 1959, p. 47.)

(5) As mentioned above and shown in the next section, "Replacement Physics," dissolution-precipitation cannot account for the properties of replacement. But dissolution-precipitation also cannot account for the fact that the dolomitization front in the field is often sharp, a feature shown in figures 2A and 2B. Quantitative models of dolomitization based on dissolution-precipitation (Wilson and others, 2001; Jones and Xiao, 2005) predict a transition zone between dolomitized and undolomitized limestone which is tens of meters wide, thus failing to reproduce the sharp contacts observed in the field.

III. REPLACEMENT PHYSICS

We justify here the second postulate of the new dolomitization model, that replacement takes place not by dissolution-precipitation but by guest-growth-driven pressure solution of the adjacent host. Throughout this paper the term *replacement* refers to the striking phenomenon identified petrographically already by Lindgren (1912, 1925) in many rocks and superbly discussed by Bastin and others (1931), whereby a crystal or crystal aggregate of a new mineral A, the guest, occupies the very space occupied before by the host mineral B, but preserving B's volume and (some) morphological details of B.

This section may be seen as a digression from our main objective—the dynamics of dolomitization—but it is a necessary digression, because it deals with the fundamental problem of the mechanism of replacement. Our discussion here, a summary from a review in progress, is based on four crucial papers: Bastin and others (1931), Maliva and Siever (1988), Dewers and Ortoleva (1989), and Nahon and Merino (1997). Others also relevant are those by Carmichael (1987), Merino and others (1993), Merino and Dewers (1998), Fletcher and Merino (2001), Merino and Banerjee (2008), and Banerjee and Merino (2011).

In a remarkable paper whose insights would be soon forgotten, Bastin and others (1931) saw that the preservation of volume and morphological details of the host by the guest that are characteristic of replacement (a) requires guest growth and host

dissolution to proceed simultaneously and at the same volumetric rate as each other; and (b) rules out formation by "dissolution-precipitation." As Bastin and others (1931, p. 603) put it,

> "Idiomorphic replacement is . . . illustrated by figures 11 and 12, which show cubic crystals of pyrite transecting the schistosity of a fine-grained schist. Obviously the pyrite [grew] by the simultaneous replacement of the several minerals of the schist. A further implication not generally recognized is that the several minerals of the schist must have been replaced at essentially the same *rate,* an astonishing fact in view of the diverse solubilities of these several minerals under most circumstances." (Bastin and others' italics; text in brackets added.)

Geochemists and modelers, however, still generally assume that replacement results from dissolution-precipitation (see below, *Geochemistry's Blind Spot*), not realizing that dissolution-precipitation cannot bring about (except by chance) the equalization of rates that Bastin and others grasped, or that there is solid petrographic evidence that rules out dissolution-precipitation as the mechanism of replacement. We see some of this evidence in figure 1A. The rhombohedral crystal of dolomite in the center has replaced the right end of the round calcium carbonate oölite at left, preserving, undeformed, its ring of black carbonaceous inclusions, thus also preserving mineral volume, since the ring of dust has not been swollen or shrunk upon growth of the dolomite. If the replacement had taken place by dissolution-precipitation, (1) the carbonaceous dust ring of the oölite would have been destroyed before the dolomite rhomb could have grown and preserved it. (2) Also, the calcitic oölite could not have dissolved leaving a hollow space having the characteristic crystal form of the future dolomite idiomorph. (3) And also: even if the oölite had dissolved leaving a hollow space with the form of the future dolomite idiomorph, and if we note that the one idiomorph replaces portions of *three* separate oölites at once, formation of the replacement by dissolution-precipitation would have required the three oölites to coördinate their respective euhedral dissolutions such that the three voids were oriented making up only *one* euhedral void that could be later filled by only *the one* dolomite idiomorphic crystal. This is impossible. Each of the three criteria present in this photomicrograph independently rules out formation of the replacement by dissolution-precipitation. "The criteria of replacement are many . . . The alert observer will discover and use other criteria of relative age and replacement [in other rocks]" (Pettijohn, 1957, p.112); see more examples in Merino and Dewers (1998).

In any case, it was clear to Bastin and others (1931) that there are genuine cases of dissolution-precipitation, that is, cases in which a mineral grain dissolves and a new one precipitates later in part or all of the space freed, but they were clear that these were not cases of replacement, because neither morphological details nor mineral volume could be preserved, since host dissolution and guest growth could not be simultaneous, nor could their rates be mutually equal (except by chance):

> "In other instances, however, minerals are dissolved by one solution and after an interval during which open spaces exist, new minerals are deposited in these spaces . . . This is *not* replacement." (Bastin and others, 1931, p. 595; their italics.)

But as noted, Bastin and others' (1931) insights were soon forgotten, and the next improvement in understanding replacement did not come until decades later, when Maliva and Siever (1988) proposed that replacement happens not by dissolution-precipitation but because of the force of crystallization exerted by the growing guest on the host. Dewers and Ortoleva (1989) applied the Navier-Stokes equation for momentum conservation to demonstrate that growth in a rigid rock must trigger other mineral reaction(s) such that volume is conserved; they thus demonstrated theoretically the existence of the replacement phenomenon. Fletcher and Merino (2001)

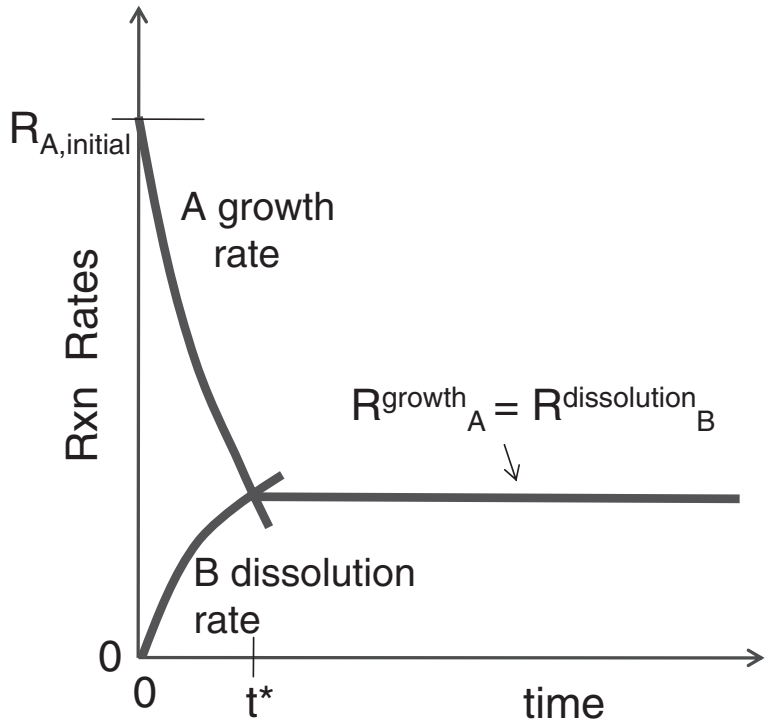

Fig. 3. How the volumetric rates of guest growth and host dissolution become automatically equalized by the induced stress (from Nahon and Merino, 1997), explaining why replacement preserves mineral volume. Driven by supersaturation, the A guest mineral starts to grow within the host rock B at its unconstrained rate $R^A_{initial}$. It soon starts to press on the adjacent B host, which is initially in equilibrium with the pore fluid ($R_B = 0$ at time zero). B starts to be pressure-dissolved by the growing A. The crystallization stress between A and B increases, and so do therefore the equilibrium constants for the two minerals, K_A and K_B, simultaneously causing the A growth rate ($\approx k_A[(Q_A/K_A) - 1]$) to decrease and the B host dissolution rate ($\approx k_B[1 - (Q_B/K_B)]$) to increase, until the two rates intersect, becoming mutually equal, at a time t^*. From then on, the two rates remain equal, and mineral volume is thus automatically preserved. The crystallization stress during replacement was calculated by Merino and others (1993) and Fletcher and Merino (2001) for several A,B mineral pairs.

showed that the correct coupling factor required for the equalization of volumetric rates in replacement was the *crystallization stress* or *induced stress,* which *can* enter into a feedback with the rates of guest growth and host dissolution, whereas the empirical force of crystallization cannot. Nahon and Merino (1997) showed how the rates are made to become mutually equal by the crystallization stress (fig. 3). The key feedback arises because the crystallization stress generated by guest growth within a (rigid-enough) rock increases the equilibrium constants of both host and guest. Through the appropriate mass-action-law expressions for host and guest, see the caption to figure 3, this causes the guest growth rate to decrease but the host dissolution rate to increase, until the two rates become equal, and thereafter remain equal during the completion of the replacement. That automatic equalization of rates has been inserted by Banerjee and Merino (2011) in their quantitative reaction-transport model of the replacement of limestone by kaolinite in the genesis of *terra rossa* (see the Discussion), leading to predicted rates of *terra rossa* formation of the same order of magnitude as paleomagnetically derived ones.

Preservation of morphological details, or "ghosts".—The preservation or erasure of morphological details by replacement can be understood if we regard the increments

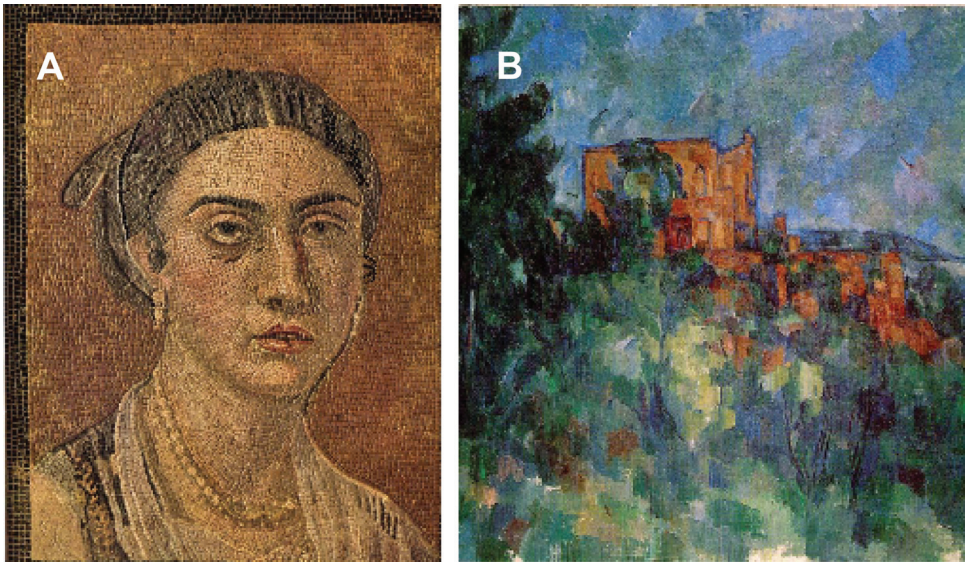

Fig. 4. Preservation and erasure of morphological details of host mineral upon replacement by pressure solution by the guest. See text. (A) The tiles representing the guest mineral's "growth increments" were so small in this mosaic from Pompeii that it was possible for the artist to capture the features of the woman's face. Photo downloaded with permission from http://www.unisa.ac.za/contents/faculties/humanities/classical/images/20.jpg, the web site of the University of South Africa. (B) The brush strokes representing "growth increments" are so large in Cézanne's "Château Noir" that we can only barely tell that the château has windows and that the foreground consists of big trees; morphological details start to become erased. Photo downloaded from the public-access WebMuseum, http://www.ibiblio.org/wm/paint/auth/cezanne/chateau-noir/chateau4.jpg.

of A growth as small tiles that pressure-dissolve their way into B. If the tiles are smaller than a detail, which is equivalent to the A growth rate being sufficiently small, then the replacement can preserve it. In the Pompeii mosaic in figure 4A the tiles used were so small that it was possible to capture the features and expression of the woman's face. In contrast, if the increments of A growth, represented by tiles or brush strokes, are as large as the details or larger, these are bound to be erased or half-erased upon replacement. In Cézanne's "Château Noir," figure 4B, the brush strokes are so large that we can only barely tell that the château has windows, and that the foreground consists of big trees.

Preservation of ghosts seems to us impossible to explain if replacement is thought to happen by dissolution-precipitation, because precipitation of the guest could not happen simultaneously with, and at the same place as, and much less at the same volumetric rate as, the dissolution of the host, except by chance or by experimental design.

Geochemistry's blind spot.—Weyl (1959), Garrels (1960), Garrels and Christ (1965), Helgeson (1968), and Helgeson and others (1969) constructed a new, quantitative geochemistry in the 1960s, long after the insights of Bastin and others (1931) had been forgotten. Weyl (1959), in his influential article proposing the idea of modeling water/rock interaction essentially by dissolution and precipitation of minerals enabled by transport in aqueous solution, was unaware of the help petrography may provide:

> "In subdividing our field, . . . we are not interested in what [a rock is like] now, but in how it became that way. . . . *Instead of looking at a rock* and asking for an explanation of its past. . . ." (Weyl, 1959, p. 2001; italics and insert in brackets are the authors')

The new geochemistry implicitly viewed every geochemical process taking place in rocks, from weathering to metamorphism, as resulting simply from dissolution and precipitation, as though in a fluid medium. Harker's (1950, p. 29) observation,

> ". . . the crystallization or recrystallization of minerals in metamorphism proceeds, not in a fluid medium, but *in the heart of a solid rock,* an environment which cannot fail to modify greatly their manner of growth" (Harker's italics),

also went unnoticed.

Thus the new geochemistry was born with a blind spot: It was unaware of the replacement phenomenon and of its fundamental kinetic implications, which could only be grasped precisely by "looking at rocks," as Bastin and others (1931) and Bastin (1950) had already done. When the problem of the replacement mechanism arose explicitly later, geochemists and modelers have continued to take for granted that replacement forms by dissolution-precipitation, unaware of the blind spot. To many geochemists (Putnis, 2009, and articles therein) the term "replacement" seems to designate whatever takes place by dissolution-precipitation, in their experiments and/or in nature, and every process from weathering to metamorphism is assumed to result from dissolution-precipitation. As we have seen, however, the term replacement already has since the early 1900s a different, far more specialized meaning: it refers to a unique kinetic-rheological phenomenon which occurs in many sorts of rocks, which is characterized by preserving mineral volume and morphological features of the host, which cannot take place by dissolution-precipitation, and whose existence—only in rigid enough rocks—was predicted theoretically by Dewers and Ortoleva (1989).

IV. NEW DOLOMITIZATION MODEL

1. The Dolomitizing Brine

As noted in the Introduction, if the brine were supersaturated with dolomite from the start, as widely assumed in the dolomitization literature, then any kind of rock could in principle become dolomitized, not only limestone as is the case worldwide. Thus in the new model the dolomitizing fluid is hypothesized to be a hot $CaCl_2$ brine rich in Mg^{2+} but undersaturated with both dolomite and calcite, and thus barren or very poor in carbonate.

Our choice of dolomite-undersaturated dolomitizing brines may seem counterintuitive at first, but it will become clear that it does trigger dolomitization only of limestones (and other rocks rich in $CaCO_3$). If the dolomitizing brine also contains chemical elements such as Zn, Pb, Fe, Sr, Ba, and sulfate, needed to make typical MVT minerals, then, as will become apparent later, dolomitization may be accompanied by formation of MVT ore deposits—which are well known to be hosted in burial dolostones.

We do not know how our postulated brines would form in nature, but, intriguingly, the deep sedimentary brines from the central Mississippi Salt Dome basin (Kharaka and others, 1987), and also the deep brines of the Smackover Formation in Arkansas (Moldovanyi and Walters, 1992), which abound in precisely the elements needed to make Mississippi Valley type ore deposits, are according to those two reports Mg-rich and slightly undersaturated with both calcite and dolomite (see table 1). In other words, these brines from the Gulf Coast basin might be natural examples of our postulated dolomitizing brines and at the same time provide a clue to why MVT ore deposits are typically associated with burial dolomites. A word of caution: The slight undersaturation with calcite and dolomite reported by Kharaka and others (1987) and Moldovanyi and Walters (1992) for the brines of table 1 depends on how the distribution of aqueous species was computed; how the pH at the *in situ* temperature was computed for each brine; which thermodynamic database was used; and, in

TABLE 1

Brines from the Central Mississippi Salt Dome Basin (Kharaka and others, 1987) and the Smackover Fm of Arkansas (Moldovanyi and Walters, 1992)

	Central Mississippi brine 84-MS-11	Smackover Fm brine 55
Depth, m	3486	2365
Temp, °C	102	85
Density, g/cm^3	1.22	1.225
Tot salinity, mg/ℓ	320,000	336,492
Li	35	37
Na	61,700	77,325
K	990	893
Mg	3,050	4,265
Ca	48,600	41,225
Sr	1,920	2,201
Ba	60	41
F	1.5	19
Cl	198,000	203,003
Br	2,020	6,647
Alkalinity	206	~100
SO_4	64	128
Mn	212	79
Fe	465	100
Pb	70	40
Zn	243	143
SiO_2	27.8	41
pH	5.08[3]	5.08[4]
S.I.(dolo)	-0.37[2]	-0.37[2]
S.I.(calc)	-0.20[2]	-0.28[1]

All concentrations are in mg/ℓ, S.I. = saturation index.
[1] Calculated with PHREEQC; http://wwwbrr.cr.usgs.gov/projects/GWC_coupled/phreeqc/
[2] From Kharaka and others (1987) and Moldovanyi and Walters (1992).
[3] In situ pH values calculated by Kharaka and others (1987, p. 557).
[4] Measured field pH, Moldovanyi and Walters (1992, table 3), who give also calculated in-situ pHs of 6.26 and 6.19 in their table 5 for this same brine.

particular, whether the reported pH was calculated taking account of internal consistency issues (Merino, 1979)—a delicate problem whose discussion is beyond the scope of the present paper.

2. *The Trigger Reaction: Fast Limestone Dissolution*

We adopt a rectangular model system consisting of porous limestone, and assume that the Mg-rich, dolomite- and calcite-undersaturated brine enters through the left side at some velocity (injected by tectonic squeezing of the deep basin or some other cause). Since it is undersaturated with calcite, the brine should first quickly dissolve some calcite according to

$$CaCO_{3(calc)} + H^+ = Ca^{2+} + HCO_3^-, \quad (1)$$

thereby producing some dissolution porosity at the entry into the current limestone "slice," between times *a* and *b* in figures 5A and B. This is why burial dolostones always

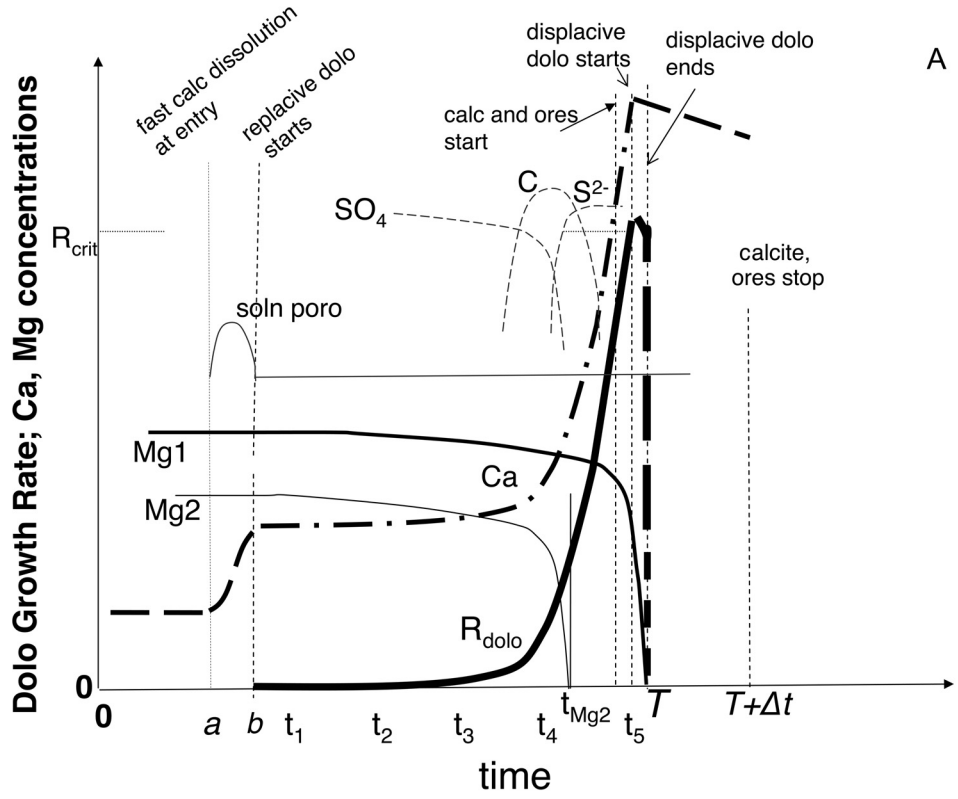

Fig. 5. Predicted dynamics of one "pulse" of dolomitization + mineralization by the postulated dolomitizing brine as it infiltrates a limestone. (A) Schematic dissolution porosity, rate of dolomite-for-calcite replacement, and concentrations of Mg, Ca, SO_4, reduced C, and sulfide concentrations, all versus *time*. Initial fast dissolution of limestone by the brine takes place between times *a* and *b*, opens a local solution porosity high, raises aqueous Ca^{2+} and CO_3^{2-} (heavy dash-dot curve), and supersaturates the brine with dolomite. Dolomite starts to grow at time *b*, replacing limestone downflow. Positive feedback between Ca^{2+} and dolomite-for-calcite replacement rate makes both quantities grow exponentially (App. 1). If and when (say, at time t_5) the dolomite rate reaches a high enough value, $R_{critical}$, taken from figure 8A, the replacive growth of dolomite becomes displacive *continuously* over a minute distance (figs. 1C-D, E-F), aqueous Mg^{2+} plummets (at time *T*), and displacive dolomite growth abruptly ends. Even before this rheological transition is reached, that is, even before time t_5, the pore fluid becomes very concentrated with Ca^{2+} so that calcite and Ca^{2+}-bearing minerals may now form. Also sulfides may now form, if sufficient organic C was released during the replacement of organic limestone to reduce sufficient sulfate to sulfide, see the speculative SO4, C_{org}, and S^{2-} dashed curves (Thom and Anderson, 2008). If the initial Mg concentration in the brine was not high enough, as in curve Mg2, then the displacive growth phase is not reached. Curved dolomite crystals are predicted to form only when Ca^{2+} becomes so high (say, at a time slightly before t_5) that it starts substituting for Mg in the structure of the growing dolomite (see text), regardless of whether the displacive growth phase is going to be reached or not.

have considerable porosity, shown in the figures as a porosity peak. But most importantly, the fast initial dissolution of some calcite at the entry point suddenly releases considerable Ca^{2+} and carbonate to the Mg-rich brine, which now becomes supersaturated with respect to dolomite. This is the key contribution of any limestone to its own dolomitization; this is why only limestones (and also siliciclastic rocks cemented with abundant $CaCO_3$) can be dolomitized. In short, the postulated calcite-undersaturated brine accounts for dolomitization *only* of limestones, for the high dissolution porosity of dolostones, and for supersaturating itself with respect to dolomite.

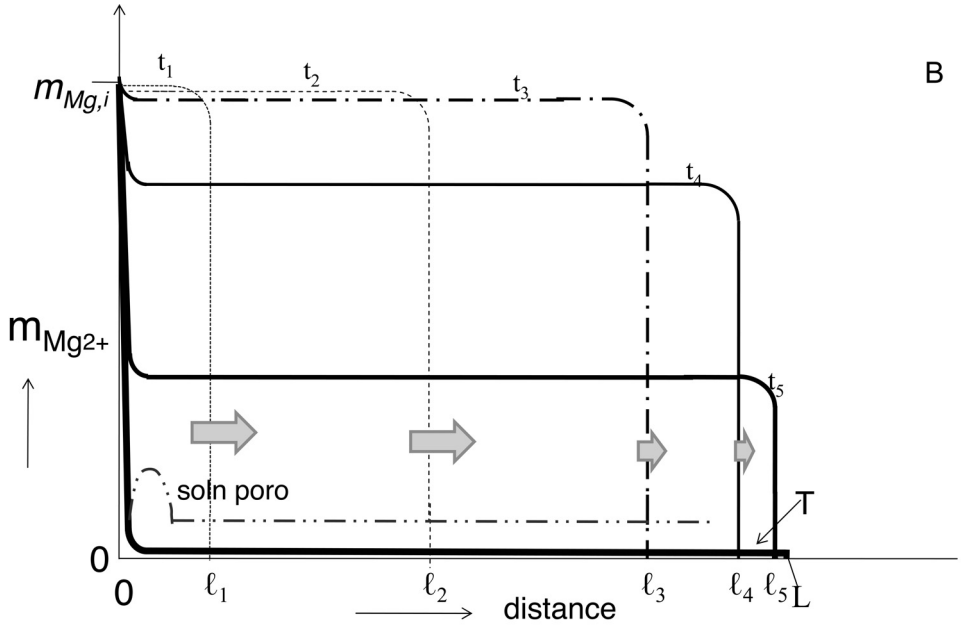

Fig. 5. (continued) (B) Schematic graph of solution porosity and Mg concentration profiles versus *distance,* at different times during one pulse. Until time t_3, the Mg concentration profiles remain high because dolomite growth is too slow to bring them down appreciably. But between times t_4 and t_5 dolomite growth accelerates exponentially (see A), Mg concentration decreases very fast and is used up at time T over the length $vT = L$, the thickness of the current reaction zone. After the crystallization of the pulse shown, hundreds more take place automatically—see text and figure 6.

3. Crucial Feedback: Self-Accelerating Dolomite-for-Calcite Replacement

At time *b* in figure 5A, the Mg-rich solution, having just become dolomite-supersaturated, starts precipitating dolomite according to

$$Ca^{2+} + Mg^{2+} + 2CO_3^{2-} = CaMg(CO_3)_{2(dolo)} \quad (2)$$

as it infiltrates through the limestone. As it grows, the dolomite pressure dissolves (thus replaces, see Section III) an equal volume of adjacent calcite according to

$$CaCO_{3(calc)} = Ca^{2+} + CO_3^{2-}. \quad (3)$$

Note that the dissolution (3) is driven by the induced stress generated by dolomite growth, not by chemical affinity as (1) was. The local mass balance of the two simultaneous, adjacent, induced-stress-coupled reactions (2, 3) is

$$1.74CaCO_{3(calc)} + Mg^{2+} + 0.26CO_3^{2-} = CaMg(CO_3)_{2(dolo)} + 0.74Ca^{2+}, \quad (4)$$

where 1.74 = ratio of dolomite to calcite formula volumes, 64.3 and 36.9 cm^3 respectively.

How and why replacement systematically conserves volume is explained in figure 3 and Section III "Mineral Replacement."

The aqueous Ca^{2+} released to the pore fluid by each increment of replacement (4) must increase the local ion-activity product and saturation index for dolomite,

$$\Omega = Q/K_{eq}^{dolomite} = (a_{Ca2+})(a_{Mg2+})(a_{CO3})^2/K_{eq}^{dolomite}, \quad (5)$$

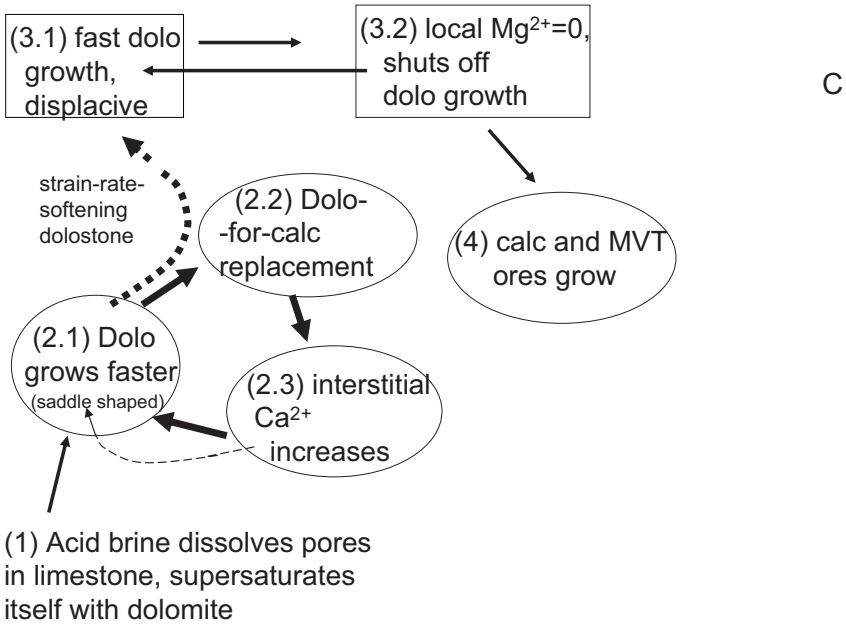

Fig. 5. (continued) (C) Flow chart of reactions, feedbacks and dynamics involved in one pulse of dolomitization. Box (1) is the initial reaction, calcite dissolution by incoming calcite-undersaturated brine, which kicks off the self-accelerating replacement described in Boxes (2.1-2.3), which in turn forces a transition from replacive growth to displacive vein dolomite growth, which shuts itself down, Boxes (3.1 and 3.2). Calcite and MVT ore growth is shown to follow, Box 4, but in fact can start before dolomite growth goes displacive.

which in turn must accelerate the growth rate of the next increment of dolomite growth, since

$$R_{dolomite} \approx k_{dolo} S_0 (\Omega - 1). \tag{5a}$$

Note that, although each increment of replacement consumes some carbonate, the CO_3^{2-} activity is probably kept roughly constant by bicarbonate dissociation. Likewise, the Mg^{2+} concentration also probably remains roughly constant in space during the advance of the brine (say, between times t_1 and t_4 in figs. 5A and 5B), because over that time interval the Mg^{2+} advection rate is much larger than the rate at which Mg^{2+} is being sequestered by dolomite growth. The strong positive feedback, shown in boxes 2.1–2.3 of figure 5C, forces both the pore-fluid $Ca^{2+}_{(aq)}$ concentration and the dolomite-for-calcite replacement rate to increase exponentially with time (see Appendix 1), as shown in figure 5A. Eventually, around time t_4, the dolomite growth rate starts to soar, soon overwhelms the Mg advection flux, and abruptly causes the Mg^{2+} to plummet between times t_5 and T—which shuts down the replacement suddenly. T is thus the time needed for the replacement rate to become so fast that it uses up all the available Mg instantaneously. By time T the replacement (of only a small fraction of the limestone, see below) has taken place over an interval of length $L = vT$, where v is the brine infiltration velocity. This is the reason dolomitization takes place by "pulses" of limited length. A tentative calculation of time T and length L are given in the next section. See Glossary, table 2.

TABLE 2

Glossary of terms used

Filling, or "packet": Mg-rich brine contained in the pores of one limestone slice, length L.
Pulse: each self-accelerating and self-shutting spurt of growth of dolomite (+calcite + ores) that takes place over a limestone thickness L, the length travelled by the brine in the time (T) that it takes for the exponential rate of dolomite-for-calcite replacement to become so fast that it uses up all available aqueous Mg abruptly.
Slice: limestone volume of thickness L in the direction of the infiltration flow which becomes completely dolomitized (by many automatically repeated growth pulses) before the reaction front jumps to the next slice.
Reaction front: space in which dolomitization of a slice is taking place currently, by repeated pulses. It remains stationary during the hundreds of pulses needed to dolomitize each slice completely; then it jumps forward to initiate the dolomitization of the next limestone slice.

4. Complete Dolomitization of a "Slice" and the Jumping Reaction Zone

The first pulse of precipitation just described can replace only a volume fraction of the current limestone slice equal to $\phi c_{Mg} b$ (see Appendix 2). Even for a brine with 10^4 ppm of Mg^{2+} and a limestone with porosity 0.2, this volume fraction would amount to only 0.005. What happens immediately after the first precipitation pulse suddenly ends, as the brine continues to infiltrate the limestone? How does the unreplaced 99.5 percent limestone in the slice become completely dolomitized—as we know it does from the sharp contacts seen in the field (fig. 2)? We see next that complete dolomitization of a limestone slice takes place by an automatic sequence of many pulses.

At time T the brine in the pores of interval $(0,L)$ in figure 5B is left completely depleted in Mg^{2+} but calcite-supersaturated. Fresh Mg-rich calcite-undersaturated brine continues to enter through the limestone cross section at $x = 0$, see figure 6. Because there is still 99.5 percent by volume of limestone left, the fresh brine immediately dissolves some calcite, supersaturates itself with dolomite, and proceeds to deposit a second pulse of dolomite precipitation similar to the first. This repetitive process continues for as long as there is *some* undissolved calcite left in the $(0,L)$ interval. $N = 1/\phi c_{Mg} b$ pulses are needed to dolomitize one slice completely, taking roughly a total time NT. It will be seen later that each pulse consists mainly of replacive dolomite, but also of very minor calcite and ores (see Section IV-7); the many thin layers of which bothryoidal aggregates of sphalerite typically consist (fig. 7A) might be seen as a record of the repeated pulses of precipitation. Tentative values of T (<100 years), L (several meters), and N (a few hundred) are calculated in Appendix 2, table A1.

This is how each limestone slice becomes completely dolomitized—in a time $NT <$ 20,000 years—before the replacement zone jumps to the next slice. In figure 6 each pulse has been represented by its exponential replacement rate versus time; only four (should be a few hundred) pulses are shown, versus time, for each of the two slices that have been already completely dolomitized—and only one for the slice currently under dolomitization. All these exponential curves and their abrupt stops are similar versions of the rate curve in figure 5A. Dolomitization of the current slice of limestone starts only after the second slice became completely dolomitized, and after a dead time T

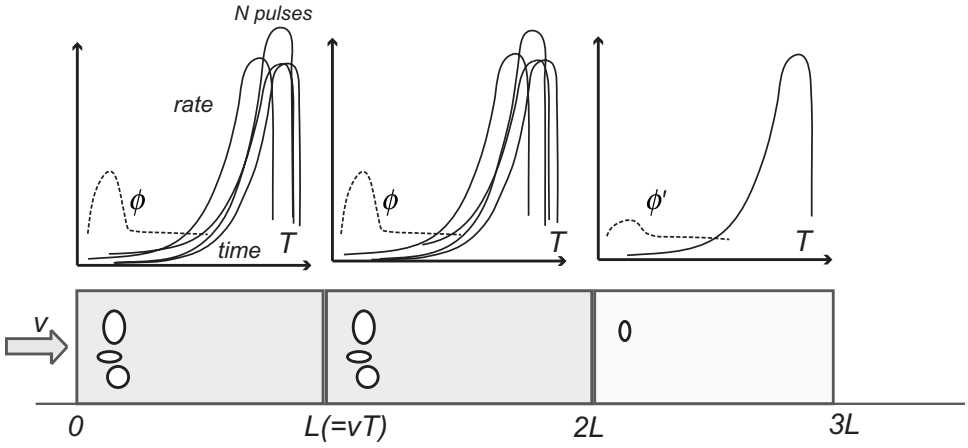

Fig. 6. Many similar pulses of crystallization of dolomite (+calc ± ores), each shown by its self-accelerating replacement rate-vs-time curve (fig. 5A), are predicted to take place automatically to replace completely each limestone slice, of thickness L. Pulses of dolomite growth keep taking place in the same slice as long as the continuously infiltrating brine finds any unreplaced limestone near the entry point. The dissolution porosity, shown by ovals, thus tends to be concentrated at the entry to the slice. In this sketch slices $(0,L)$ and $(L,2L)$ have been completely dolomitized (by a few hundred growth pulses each, though only four are shown). Dolomitization of the next slice $(2L,3L)$ has just started.

during which fresh Mg-rich brine flows through the slice just dolomitized—without reacting with it—and starts entering the next slice at $x = 2L$. The reaction zone now jumps forward by a distance L to its next position, $(2L,3L)$ in figure 6, where it will remain for the next NT years.

The final phase of each pulse (especially for the latest several pulses of each slice), when the dolomite growth reaches its greatest rate, is a moment of particular activity and complexity. There may occur a self-induced change in the rheology of the local dolostone; this is discussed in Sections IV-5 and IV-6. Several minerals grow in this final phase, during and after the dolomite shutdown, that constitute a characteristic paragenesis in burial dolostones; this mineralization is described in Section IV-7.

5. From Replacive to Displacive Growth: Self-Induced Change in Dolostone Rheology

The self-accelerating dolomite-for-calcite replacement ends up—if aqueous Mg^{2+} is not used up first—modifying the rheological response of the crystalline dolostone to the crystallization stress, or induced stress, generated by dolomite growth. The property that makes this possible is that crystalline carbonates are non-newtonian materials of the strain-rate-softening kind (Verhoogen and others, 1970, p. 508), that is, their viscosity decreases as the carbonate is deformed at an increasing strain rate. This behavior was demonstrated experimentally by Heard and Raleigh (1972) for Yule marble at temperatures between 300 and 800 °C; their results, fitted by them to the Weertman equation, yielded

$$\dot{e} = H\sigma^N, \tag{6}$$

with a stress exponent $N \approx 8$. The stress versus strain rate curve, graphed schematically in figure 8A, is knee-shaped. The viscosity of the marble, η $(= d\sigma/d\dot{e} = G\dot{e}^{-7/8})$, equal to the slope of the curve at each point, obviously decreases with increasing strain rate, expressing that marble is indeed strain-rate-softening in the temperature ranges studied. [e is strain, $\dot{e}$ is strain rate $(= de/dt)$, σ is stress, and H and G $(= H^{-1/8})$ are temperature-dependent factors.] We assume that this strain-rate-softening behavior

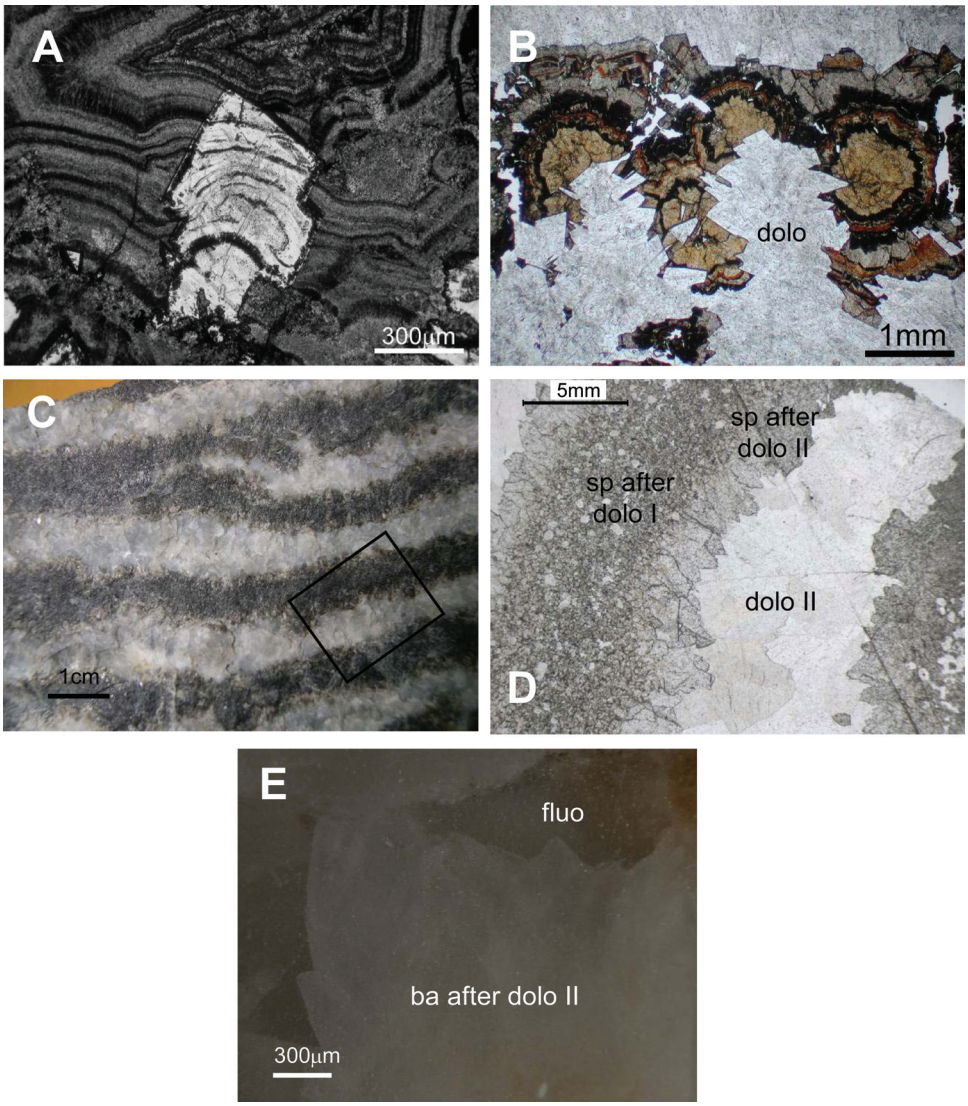

Fig. 7. Replacements among dolomite and ores in burial dolostones. (A) A curved dolomite rhombohedron replaces sphalerite at the Galmoy ore deposit, Ireland, preserving the layering of the disappeared sphalerite. (B) Dolomite replaces botryoidal sphalerite at Riopar, Albacete (Spain). (C) Sphalerite partly replaces dolomite leaving unreplaced the central portion of each zebra vein, at San Vicente, Peru. (D) Plane-polarized view under low magnification of the area marked in (C). Note that the medium gray sphalerite preserves rhombohedral terminations and cleavages of displacive dolomite-II, one of them curved; the sphalerite preserves both the small crystal size of the replacive dolomite-I, and the large crystal size of the displacive dolomite-II. (E) Barite at center replaces a curved dolomite-II crystal at the Hammam Zriba deposit (Zaghouan province, north-eastern Tunisia). The dark gray areas at top right and left are fluorite replacing displacive dolomite.

applies also to crystalline dolostones, and down to the 300 to 100 °C range of relevance to burial dolomitization. The mechanism of dolostone deformation at this low temperature range is non-pervasive volume loss by pressure solution at stylolites, as shown by Merino and others (2006).

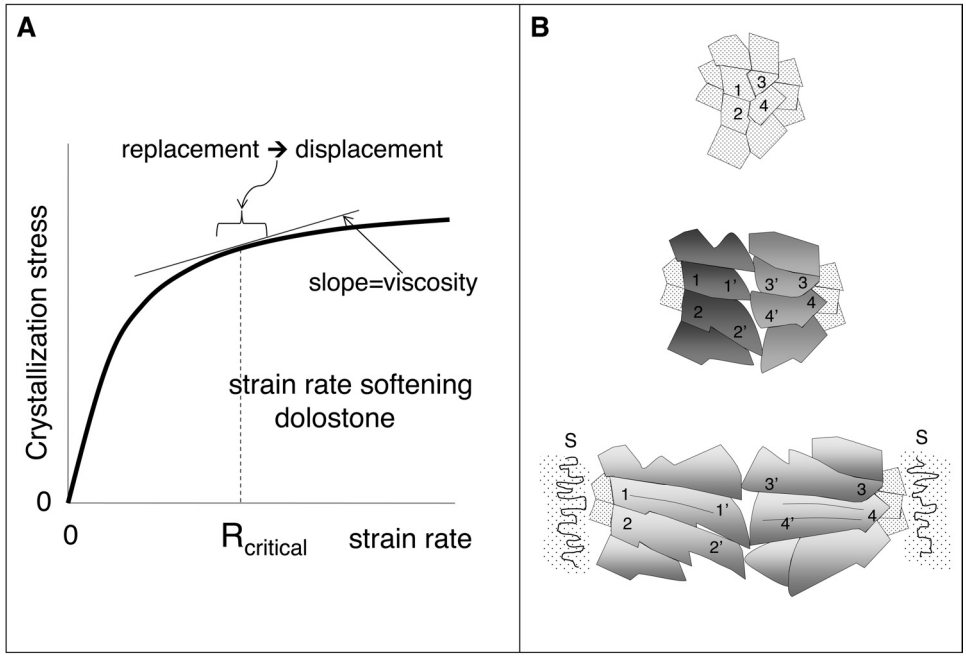

Fig. 8. (A) Schematic graph of strain-rate-softening dolostone (eq 6): because the dolomite-for-calcite replacement is self-accelerating, the dolomite growth rate, which is equivalent to the strain rate generated by the dolomite growth, increases during replacement and must reach a critical value R_{crit} for which the rock viscosity (=slope of curve) becomes low enough to let the until-then replacive growth pass *continuously* into displacive, naturally causing the contact between replacive and displacive dolomite to be gradual and seamless—as sketched in figure 8B and as observed petrographically (figs. 1C,D and E,F). (B) Predicted growth of one displacive dolomite vein; see text. *Top:* Dolomite (stippled) has just replaced calcite crystals 1–2 and 3–4 reaching a rate sufficiently high to trigger the transition to displacive growth shown in the next frame. *Middle:* The now-displacive dolomite crystals 1–2 and 3–4 have grown towards each other. Each crystal consists now of a replacive portion (such as 1 or 4) and a displacive portion (such as 1′ or 4′), with no interruption of growth (and thus, no sharp contact) between the two. The two portions are in structural continuity. The structure is curved because of increasing Ca-for-Mg substitution and/or incorporation of submicroscopic slivers of calcite within the dolomite. The displacive growth generates a vein that extends at right angles to the growth, that is, vertically in the figure. *Bottom:* the displacive growth, necessarily very fast and short lived, has just ended. The displacive portion of each crystal is deformed. Small voids are left in the middle of the vein between the subhedral terminations of the displacive crystals. The thickening of the vein pushes outward and generates stylolites (S) in the dolomite-I walls. See Merino and others (2006) for the induced-stress feedback between neighbor parallel veins that makes them equidistant.

The combination of self-accelerating replacement and strain-rate softening dolostone has a surprising consequence. Since the self-accelerating replacement imposes—via the crystallization stress exerted by the growing dolomite—an ever-increasing (elastic) strain rate on the host dolostone itself, it follows (fig. 8A) that the dolostone's bulk viscosity must decrease rapidly as the replacement self-accelerates past the elbow in the stress-versus-strain rate curve, and perhaps especially so in the latest several pulses of the slice, when the slice is really a crystalline dolostone texturally similar to the marble on which Heard and Raleigh (1972) carried out their experiments.

Thus, when the slice is sufficiently crystalline (in late pulses) and its viscosity is lowered sufficiently—that is, when the dolomite growth rate and thus the strain rate reach a high enough value $R_{criticab}$ figures 5A and 8A—the dolomite growth should pass continuously from replacive to displacive, as sketched in figure 8B. The replacive crystals 1, 2, 3, 4 (fig. 8B) that happened to be growing at time t_5 (see fig. 5A)—when the rheological transition takes place—would each consist of a replacive portion

(formed just before t_5) and of a displacive portion (1′,2′,3′,4′) grown between times t_5 and T) with no sharp boundary between them, and with the displacive portion in optical continuity with the replacive portion, as shown in figure 8B. The forced displacement of 1,2 from 3,4 will propagate sideways, resulting in a bilateral, syntaxial vein. Many such displacive veins would be simultaneously generated over tens of centimeters or more; their orientation and interactions were studied by Merino and others (2006)—see next section.

6. Displacive Veins of Saddle Dolomite

Gradual, seamless contact bewteen dolomites I and II.—The predicted seamless, optically continuous displacive crystals and vein growth just described exactly match the two examples shown in figures 1B, 1C and 1D, 1E as well as those reported by Tona (ms, 1973), Fontboté and Amstutz (1980), Horton (1989), Wallace and others (1994), Gasparrini (ms, 2003, plates 8, 9), Vandeginste and others (2005), Gasparrini and others (2006), and Merino and others (2006), who pointed out that the margins of the dolomitic zebra and breccia veins are, under the microscope, gradual (over a length of a few micrometers) and seamless.

It now becomes clear that the observed gradual transition from replacive dolomite to white displacive veins means that there was no growth interruption between them; that the displacive dolomite-II is not filling a prior void (but making room for itself by pushing the host replacive dolomite aside); and that the two dolomites form at the same temperature and from the same (though quickly evolving) aqueous solution.

Genesis of saddle-shaped dolomite.—Saddle-shaped dolomite crystals are known to be extra-calcic. Radke and Mathis (1980) hypothesized that the extra Ca substitutes for Mg in dolomite and deforms its structure, because $Ca^{2+} > Mg^{2+}$ in size. By transmission electronic microscopy Barber and others (1985) found submicroscopic bifurcating calcitic ribbons, each a few to 100 nm thick, coherently incorporated in crystals of saddle dolomite, and attributed the deformation to such microstructures. Either or both microstructures would account for the characteristic deformation of the structure that results in saddle-shaped dolomite-II crystals and for their concomitant extra-calcic composition. But what neither article solved was why those microstructures were systematically present in the dolomite-II of a burial dolostone and even in some dolomite-I crystals. Radke and Mathis (1980) thought that the proposed cation substitution might result from high temperature.

Now we realize, however, that the driving force that pushes Ca^{2+} to substitute for Mg^{2+} in dolomite crystals, and/or that forces the precipitation of submicroscopic calcitic slivers within the dolomite crystal structure, must be none other than the exponentially rising pore-fluid Ca^{2+} concentration, which is forced to reach very high values by the same feedback that forces the replacive dolomite growth rate to become huge and—if the Mg^{2+} lasts—to seamlessly transition into displacive growth. This is why the fastest growing dolomite crystals, regardless of whether they have already become displacive, are also the ones that are systematically saddle-shaped. Examples of saddle dolomites are in figures 1B, 1C and 1D, 1E.

Syntaxial, self-organized, thin displacive veins.—The displacive dolomite crystals should make up syntaxial (or bilateral) veins, as shown in figure 8B. (A syntaxial vein consists of crystals that grow inwards from each side and that are in optical continuity with crystals of the same mineral from the walls; the vein ends up having a center seam.) At time t_5 in figure 5A many such incipient displacive veins would start to grow within the reaction zone. The orientation of the veins was predicted by Merino and others (2006): If the principal stresses are mutually equal the incipient veins tend to be oriented randomly, and upon further growth they intersect each other and generate a so-called “breccia” texture. If the principal stresses are slightly unequal the veins tend to orient themselves normal to the least stress, generating a zebra texture, or rhythmite

(figs. 1B-C, 1D-E, and 7C,). In this case the induced stress exerted by the veins as they thicken (1) should generate stylolites (marked "S" in fig. 8B) in the slice of the host dolomite-I caught between adjacent veins, and (2) should trigger a feedback that by pressure-solution "weeds out" veins that are too close to their neighbors, with the survivors of this *triage* being left more equidistant than before (Merino and others, 2006).

But this displacive dolomite growth phase cannot last long. The transition of replacive to displacive only happens if and when the rate of dolomite-for-calcite replacement reaches a high enough value, $R_{criticab}$ that corresponds to the strain rate for which the dolostone's viscosity becomes low enough for the growth to be accomodated displacively instead of replacively (fig. 5A). But as soon as the replacement transitions into displacement, pore fluid Ca^{2+} stops being raised, which shuts off the self-accelerating feedback. The displacive dolomite continues to grow at the very high rate $R_{criticab}$ very fast scavenging all the aqueous Mg from the brine, whereupon the growth rate of dolomite itself comes down to zero abruptly. The displacive veins only have between times t_5 and T to grow, figure 5A, a very short interval because the drop in Mg and in rate is practically instantaneous relative to the infiltration velocity. Thus the veins are predicted to be thin, as observed (Merino and others, 2006).

Note that the displacive growth phase can be bypassed altogether. If the Mg^{2+} concentration in the initial dolomitizing brine is not sufficiently high, then Mg^{2+} gets used up completely—and the replacement rate is suddenly brought down to zero—before the strain-rate can reach the appropriate $R_{critical}$ value needed for the rheological transition to displacive growth discussed above. This is the case for the "Mg2" profile in figure 5A, which may explain why the thin displacive vein sets may not occur at all in some burial dolomites, or may occur only at a few, meter-sized regions within huge volumes of dolomite-replaced limestone.

7. *Mineral Paragenesis of Each "Pulse"*

We have discussed the dynamics of the replacive (±minor displacive) dolomite growth and have seen how the self-accelerating replacement automatically leads to the complete dolomitization of each $(0,L)$ slice by hundreds of pulses, before the reaction zone jumps to the next slice, $(L,2L)$. But we left out that when the self-accelerating dolomitization shuts itself down by sudden Mg^{2+} "sequestration" in each pulse, and even before, other minerals must precipitate as well. We look at these in this section. Since pore fluid Ca^{2+} concentration is necessarily very high when the Mg^{2+} concentration plummets (fig. 5A), we expect Ca^{2+} minerals to start forming immediately.

The first is calcite, which should cement the small spaces in the center seam of displacive zebra veins (see fig. 1D-E), and which should back-replace, or "dedolomitize," some of the replacive and especially the displacive dolomite just made (see figures 169, 170 in Adams and others, 1984). The new model thus naturally explains a feature—growth of so-called late-stage calcite—that had long been puzzling (Spirakis and Heyl, 1995) from the perspective of the prevailing theory of burial dolomitization. Benito and others (2006) have found what we take to be good indirect evidence of dedolomitization in the form of minute dolomite inclusions within late-stage calcite yielding an isotopic composition identical to that of nearby ferroan saddle dolomite crystals. Note that the submicroscopic calcitic slivers that form within the late, fastest-growing dolomite crystals, deforming them into saddle shapes, are driven by the same huge Ca^{2+} that drives the late-stage calcite; see section on saddle dolomites above.

Fluorite, anhydrite, barite.—If the original brine contains significant fluoride (as the brine from the Smackover Formation in table 1 does), the huge Ca^{2+} concentration reached should form fluorite, an ore commonly found in MVT deposits associated with burial dolomites, also back-replacing the host dolomite. Similarly, if the interstitial

solution contained sulfate and barium, and if this sulfate has not been appreciably reduced—see next section—then minor anhydrite and barite (fig. 7E) would also be expected to form at some place(s) within the current $(0,L)$ pulse, at around or right after time T in each pulse, the moment when Mg^{2+} becomes abruptly zeroed out in the pore fluid.

Sulfates versus sulfides.—If the brine contains base metals and sulfate (as those in table 1 do), and if the limestone undergoing replacement by dolomite contained appreciable organic matter, several sulfides—galena, sphalerite, pyrite, marcassite—should precipitate during and after the late-replacive and displacive dolomite phases. This is because the organic carbon that is released to the pore fluid by the dolomite-for-limestone replacement would reduce the aqueous sulfate to sulfide, as suggested by Thom and Anderson (2008) and Anderson and Thom (2008). The probable concentrations of sulfate, organic carbon, and sulfide versus time within one pulse of growth are shown qualitatively in figure 5A.

8. Self-Cannibalization: MVT Ores Are "Swept" Downflow

When much of the limestone slice currently under dolomitization is dolomitized, the dolomite and ores of late pulses may partly replace ores and dolomite, respectively, formed in earlier growth pulses of the slice. Several examples are shown in figure 7. Dolomite replaces ores at Galmoy (Ireland) and Riopar (Albacete, Spain), figures 7A and 7B. Sphalerite replaces dolomite I and II at San Vicente, Peru, figures 7C and 7D. Barite and fluorite replace dolomite-II at the Hammam-Zriba Mine (Zaghouan district, Tunisia), figure 7E. Fluorite replaces dolomite at Sierra de Gádor (Almería, Spain), and at the Dau Range (Carinthia, Austria), see Zeeh (1995). At the Polaris deposit (Canadian Arctic Archipelago) dolomite was dissolved o replaced by sulfide-precipitating fluids (Savard and others, 2000). For the Buick mine of southeast Missouri Sverjensky (1981) gave and cited petrographic evidence that both galena and sphalerite have precipitated and dissolved repeatedly during ore formation, and suggested that repetitive precipitation and dissolution of galena was probably an important process during the formation of the entire Viburnum Trend. We have seen above that some late-stage calcite produced at the end of late pulses may "dedolomitize" some dolomite.

As a result of all these replacements, the aqueous components released to the interstitial brine—mainly CO_3^{2-}, Mg^{2+}, Zn^{2+} and S^{2-}—are advected forward and promote reprecipitation of more dolomite and/or sphalerite and other ores downflow, generating a larger and larger ore deposit always associated with the current position of the advancing dolomitization front. This progressive accumulation of a scarce mineral at a moving reaction front was modeled quantitatively for a generic, simplified case by Ortoleva and others (1986). We have loosely adapted their dynamic model to dolomitization in figure 9, which shows that at any given time most or all of the ore formed previously (both in previous pulses of the same slice and in previous slices) accumulates at the current front. In fact Harper and Borrok (2007) have reported that the largest zinc and lead deposits of the midcontinent of the U.S. do occur at the last position of the dolomitization front, against the undolomitized limestone.

9. Geochemical Features of the Dolomite Growth

Since the displacive dolomite grows continuously on replacive dolomite, it is not surprising that they have been found to have the same or very similar geochemistry. Previous investigators supporting the "two-dolomites" model have been understandably intrigued by the observed geochemical similarity, and have endeavored to explain it. For example, Lonnee and Machel (2006) proposed that the dolomite-I is altered hydrothermally by the same solution that deposits the dolomite-II. However, the fact

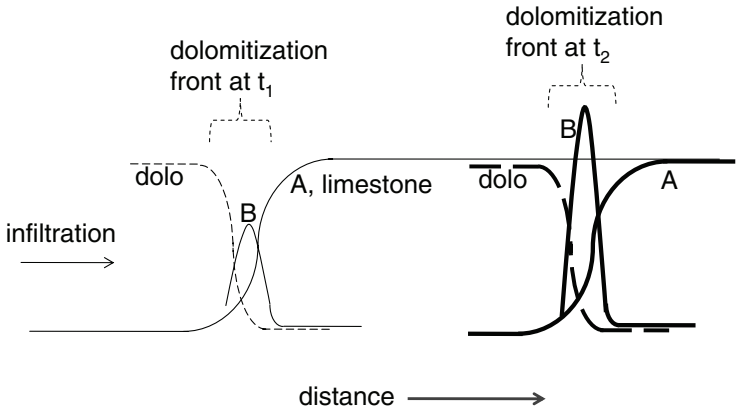

Fig. 9. Predicted self-cannibalization and "sweeping" of ores forward. Because dolomite of a late pulse may partly replace ores of previous pulses of the same slice (see several cases in fig. 7), the ores are expected to be continually "swept" forward and to accumulate in the current reaction front. The snow-plough-like accumulation of an ore (B) at the current front was modeled by Ortoleva and others (1986, their fig. 2) in a general case, adapted here to dolomitization. The predicted forward accumulation of ore appears to be confirmed by the fact that Zn deposits in the U.S. midcontinent (Harper and Borrok, 2007) are largest at the final position of the dolomitization front. Also, ore mineral grains formed in late pulses may replace a little dolomite formed in earlier pulses (as in figs. 7C-E), "sweeping" it forward too.

that the dolomite-for-calcite replacement is self-accelerating can be expected to have a differential kinetic effect on the contents of trace elements and O, C isotopes incorporated by the growing dolomite. If heavy carbonate ions, $^{13}C^{18}O_3^{2-}$, move more sluggishly than light ones, $^{12}C^{16}O_3^{2-}$ (O'Neil, 1986, p. 2), then we can expect that a dolomite crystal that grew at the high growth rate corresponding to times t_4 and T in figure 5A should have lower $\delta^{18}O$ and $\delta^{13}C$ values than another that had grown at a lower rate, say, that between times t_1 and t_4. $\delta^{18}O$ and $\delta^{13}C$ values for four pairs of replacive and displacive dolomite crystals from the dolomitized Cretaceous limestones of the Basque-Cantabrian basin are given in table 3 (Simón and others, 1999), with the replacive and displacive crystals of each pair only a few centimeters from each other, do indeed show the predicted trend: the replacive dolomite of each pair is a few permil higher than the nearby displacive dolomite crystal, which according to the new

Table 3

Comparison of $\delta^{18}O$ (‰ VSMOW) and $\delta^{13}C$ (‰ PDB) values for four pairs of nearby replacive (R, or dolomite-I) and displacive (D, or dolomite-II) dolomite crystals from dolostones in the Cretaceous Basque-Cantabrian basin, northern Spain

Sample#	$\delta^{18}O$	$\delta^{13}C$
C98-15b-R	19.2	0.2
C98-15a-D	15.5	-0.8
C98-53b-R	19.9	1.5
C98-53a-D	14.5	0.6
C98-59b-R	18.3	0.5
C98-59c-D	14.8	0.4
S98-23b-R	20.3	2.8
S98-23a-D	15.7	-2.4

Data from Simón and others (1999).
In each pair the displacive (D) crystal is isotopically lighter than the nearby replacive (R) crystal.

dynamic model grew at a much higher rate. The close proximity of the two crystals of each pair makes it unlikely that the $\delta^{18}O$ and $\delta^{13}C$ differences could be due to a temperature difference between their locations. The same trend—isotopically slightly lighter dolomite II—was found also by Fontboté and Gorzawski (1990) for the burial dolostones at San Vicente, Peru, by Gasparrini and others (2006) for burial dolostones of the Cantabrian Zone, northern Spain, and by Mattes and Mountjoy (1980).

Since the Ca^{2+} concentration in the pore fluid increases exponentially along with the growth rate, very-fast-growing dolomite crystals (those growing between times t_4 and *T* in fig. 5A) must be more Ca-rich (and thus deformed) than those that grew earlier, between times t_1 and t_4.

Similarly, the degree of trace element incorporation should differ considerably from fast-growing to slow-growing dolomite crystals that are near each other, warranting caution in dealing with trace element and fluid inclusion analyses, which should not be interpreted as reflecting equilibrium. In particular, the ratio Mn/Fe, which is thought to be one of the controls of cathodoluminescence in dolomite crystals, may be expected to vary wildly especially for the higher rates of dolomite growth at times t_4 to T (fig. 5A), potentially leading to sudden changes in cathodoluminescence in the saddle dolomites but not in nearby replacive dolomite crystals formed from the same solution. The observation that the dolomite-I and dolomite-II have different cathodoluminescence (for example, Gregg and others, 2001; Chen and others, 2004; Gasparrini and others, 2006; Lonnee and Machel, 2006; Choquette and Hiatt, 2008), could be explained by the differential effect of self-accelerating kinetics on the incorporation of Fe and Mn as traces.

The dolomite- and calcite-undersaturated, and thus very carbonate-poor, property of the dolomitizing brine—see probable analogues in table 1—suggests that $\delta^{13}C$ values of the dolostone should be determined by those of the host limestone, since the brine can contribute only negligible carbonate to the dolostone. This is borne out by the analyses of Land (1980), Montañez and Read (1992), Hitzman and others (1998), Gasparrini (ms, 2003), and Carmichael and others (2008), among others.

10. Lobed Dolomitization Front and the Reactive Infiltration Instability

The large porosity created by limestone dissolution via reaction (1) in each slice should trigger the *reactive infiltration instability,* first identified and modeled by Chadam and others (1986) and Ortoleva and others (1987b) and proposed recently to generate the funnels and sinkholes characteristic of karst (Merino and Banerjee, 2008). The dissolution porosity created in each position of the reaction front attracts additional brine flux, which in turn carries out faster the dolomitization reactions described in this chapter, increasing faster the creation of further new dissolution porosity, thus permeability. The basic consequence of this instability (for example, Wei and Ortoleva, 1990; and Aharonov and others, 1997) is that the reaction zone, even if initially planar, tends to become fingered in the general direction of the brine's flow. Then the competition for reactive flux continues among the fingers themselves, leading to successive jumps in the size and spacing of the lobes (Szymczak and Ladd, 2006). Actual fingering of the dolomitization front has been described by Mattes and Mountjoy (1980) for the Miette buildup of Alberta; Wilson and others (1990) for the Latemar buildup of northern Italy; Gasparrini and others (2006) for Upper Carboniferous carbonates of the Cantabrian Zone of northwestern Spain (fig. 2A); and many others.

11. Spatial Distribution of Dissolution Porosity

Because for every pulse the initial fast dissolution of limestone takes place immediately upon entry of the calcite-undersaturated, Mg-rich brine into the current reaction zone, we expect that there would be a porosity maximum at the entry to each

limestone slice dolomitized. The small circles in the entry points of the slices already dolomitized and of the "current slice," figure 6, represent that dissolution porosity maximum. If each slice turns out to be several meters thick (see table A1, Appendix 2) then we would expect a spatial dissolution porosity periodicity of several meters. Interestingly, this prediction may be confirmed by Budd and others (2006), who have reported porosity periodicities on several scales, up to several meters, in fair agreement with tentative calculations of L in table A1.

V. DISCUSSION AND FUTURE WORK

A serendipitous discovery.—The new dolomitization model is a forward, nonlinear model that predicts a string of linked loops and cyclicities (figs. 5C and 6) and self-cannibalization (fig. 9), the whole driven by disequilibrium between the dolomitizing brine and a platform limestone. Based on two postulates and on the operation of several feedbacks, the model generates a self-organized dynamics many of whose predictions and consequences are confirmed by observation. The first postulate—that the dolomitizing brine must be Mg-rich and *undersaturated* with both calcite and dolomite—was made because, if the brine were dolomite-supersaturated as assumed in the literature, *any* rock type could in principle be dolomitized, not just limestones. The undersaturation with calcite, combined with the fast kinetics of calcite dissolution, provides the crucial "kick" to the system that starts the process (but only in limestones) resulting right away in dissolution porosity and in supersaturation with dolomite, which in turn, when combined with the self-accelerating feedback via Ca^{2+} inevitably involved in the dolomite-for-calcite replacement (Section IV-3), triggers self-organized dolomitization in both time (in the form of many repeated pulses per limestone slice) and space (in the form of successive slices). The second postulate—that replacement happens by guest-growth-driven pressure solution of the host mineral—has been justified in detail in Section III.

Remarkably, the assumed chemistry of the dolomitizing brine and the replacement physics of the second postulate, combined with the self-accelerating feedback via Ca^{2+} involved in the dolomite-for-calcite replacement (Section IV-3), and with the non-newtonian rheology of crystalline carbonates (Section IV-5), *also* accounts for a suite of heretofore enigmatic textures, microstructures, parageneses, and lithological association with MVT ores that are characteristic of burial dolostones. That suite of properties includes: the *displacive* nature of dolomitic zebra and breccia veins; a replacive/displacive contact that is systematically *seamless;* the *saddle shape* and extra-calcic composition of the displacive dolomite crystals and of the replacive crystals formed late in each pulse; the displacive veins are always thin and equidistant (by a "triage" or "weeding" feedback described by Merino and others, 2006); that the growth of dolomite must periodically shut itself down and cause immediate growth of "late-stage" calcite and ores; that the late dolomite of each pulse has lower $\delta^{18}O$ and $\delta^{13}C$ than the early dolomite; that the MVT ores tend to be concentrated in the last position of the dolomitization front; that dissolution porosity should tend to be spatially periodic. The feedback causes dolomite to grow even though Mg/Ca *decreases* during any one pulse (see fig. 5A), illustrating how disequilibrium plus feedback trumps the conventional dolomitization condition, that $Mg/Ca > K_{eq}$. The growth only stops when Mg^{2+} is abruptly and totally scavenged from the current packet, or "filling" (table 2), of aqueous solution.

All of the pieces of the new dynamics work together to form a consistent model. If any of the postulates were wrong, or if the dolomite-for-calcite replacement were not self-accelerating, or if it were not self-accelerating *via* Ca^{2+}, or if calcite dissolution were not inherently very fast, or dolostones not strain-rate-softening—the model would not work.

Self-organization.—Since the new model involves disequilibrium (between the dolomitizing brine and a limestone) and feedbacks, the two necessary conditions for geochemical self-organization (Merino, 1984; Ortoleva and others, 1987a; Merino and Wang, 2001), it is not surprising that the model predicts that dolomitization should be self-organized, and self-organized in several ways at once. First, as noted, the self-accelerating-replacement feedback leads to a temporal self-organization in the form of many successive "pulses," or spurts, of mineral growth in each "slice," even under steady infiltration. The feedback, because it couples the replacement rate and the pore fluid Ca^{2+} (Section IV.3), causes each pulse to consist of the same paragenesis, namely replacive dolomite with small amounts of ± displacive dolomite + calcite ± ores. Each pulse however replaces less than one percent of the limestone in the slice. Each pulse is triggered by the supersaturation with dolomite caused by dissolution of some unreplaced limestone by a new packet of brine. The pulses repeat themselves (probably in the hundreds, see table A1) until the current limestone slice is completely replaced, providing a straightforward way to account for the precipitation of the layered sphalerite aggregates common in MVT deposits. The predicted self-organization in the form of pulses thus makes it unnecessary to postulate repetitive seismic pumping of brine (for example, Sibson, 1994) or episodic fault-related brine flow (McLimans and others, 1980) to account for the sphalerite layering. There is also a spatial self-organization in the form of sequential "slices" with spatially periodic dissolution-porosity highs concentrated preferentially at the entry region of each slice, as shown in figure 6 and Section IV-11, explaining the porosity periodicities detected by Budd and others (2006).

Second, the rheologic-kinetic feedback described in sections IV-5 and -6, causes the replacive dolomite growth to become displacive (though only for a very short time; see fig. 5A), and this leads to the formation of sets of thin veins that if parallel become roughly equidistant through a "weeding" or "triage" feedback described by Merino and others (2006), forming the so-called zebra veins found in most burial dolomites. The zebra veins of a set are simultaneous, and do not result from repeated episodic flows.

Finally, the reactive-infiltration instability causes dolomitization to proceed in self-organized large fingers and lobes (Section IV-10).

Burial dolomitization is fast.—We deduced that both the coupled pore-fluid Ca^{2+} and dolomite-for-calcite replacement rate grow exponentially on time as the dolomitizing brine infiltrates the limestone, during each pulse (see Appendices 1 and 2). The time, T, at which the replacement rate becomes so high as to suddenly use up all the aqueous Mg^{2+} contained in the current packet of interstitial brine, denotes the duration of one pulse.[1] It is calculated with equation A7 and given in table A1 (Appendix 1) for each of two estimates of the 100 °C dolomite growth rate constant, and for a brine with 10^4 mg Mg/ℓ infiltrating a 0.2 porosity limestone at 10 cm/year. The calculated T is 5.5 and 55 years, respectively, which multiplied by the assumed infiltration velocity yield lengths L of 0.5 and 5.5 meters, respectively. (L is the predicted thickness of a slice.) Since each pulse affects only 0.5 percent of the slice, about 200 pulses (each lasting $\ll$100 years) will take place automatically[2] until the dolomitization of the slice is completed—in only <20,000 years. A faster advection velocity would proportionally increase the predicted thickness of a slice, L, without changing T. Lower dolomite rate constant and/or lower surface area increase both T and L. The new model poses no restrictions as to the type and timing of the advection

[1] This time T for simplicity neglects the time ΔT (fig. 5A) required for the growth of the late-stage calcite + ores towards the end of each pulse.

[2] Recall that each pulse is triggered by the dissolution of some limestone by fresh brine at the entry into the slice.

that brings the deep hot dolomitizing brine to a platform limestone. The predicted *fast* dolomitization implies that the dynamic process is probably essentially isothermal.

Syntaxial veins.—The new model explains physicochemically why zebra veins are displacive and how they form in burial dolomites. The zebra veins are of the kind called *syntaxial* by structural geologists. Wiltschko and Morse (2001) and Fletcher and Merino (2001) independently showed that many bilateral veins grow displacively, pushing aside their walls through the crystallization stress generated by the inward growth itself. Merino and others (2006) gave evidence that dolomitic zebra and breccia veins are indeed displacive. What the new dolomitization dynamics now shows is that the replacive dolomite-for-calcite growth, because it is self-accelerating, becomes eventually fast enough to lower the dolostone viscosity sufficiently to permit the replacive growth to seamlessly become displacive—and generating a vein oriented at right angles to its growth direction, as shown in figure 8B. The conventional view (for example, Bons, 2000)—that a syntaxial vein grows by repeated cycles of cracking and cementation, as per the so-called crack-seal mechanism—rests on the assumption that there is an exterior force that, conveniently, repeatedly cracks the rock at the place where, and at the time when, the vein is ready to grow by precipitation of cement, and does not explain why the vein consists of the same mineral as its walls, or why the contact between wall and vein is seamless.

Implications for reaction-transport modeling.—Existing quantitative models of dolomitization (for example, Wilson and others 2001; Caspard and others, 2004; Whittaker and others, 2004; Jones and Xiao, 2005; and references therein) have explored the ability of different large-scale brine flow regimes—reflux, gravity, thermal convection, tectonic squeezing, compaction—to drive dolomitization, incorporating premises of the prevailing model that we have discussed in Section II, such as that dolomitization is effected by dolomite-supersaturated brines through the mass balance 2calcite + Mg^{2+} = dolomite + Ca^{2+} or that the dolomite-I and the dolomite-II are produced by separate brines or at different times. Similarly, there are models quantifying the formation (by cooling of the ore fluid; by mixing of hydrothermal fluids; by regional brine flows) of Mississippi-Valley type ore deposits but without accounting for their association with burial dolostones (see Bethke and Marshak, 1990; Garven and others, 1993; Plumlee and others, 1995; Corbella and others, 2004; among others). We do not discuss those models here. We suggest instead that the dynamics presented here provides a blueprint of the brine chemistries, driving forces, mineral reactions, and feedbacks that should be included in future quantitative reaction-transport models of dolomitization and MVT mineralization. Crucial in such models will be to monitor the varying aqueous speciation of the interstitial brine during the precipitation of the characteristic paragenesis that constitutes each "pulse" (namely, replacive dolomite ± minor displacive dolomite + calcite ± ores, Section IV.7). The aqueous speciation should vary during each pulse because of the exponential increase in pore-fluid Ca^{2+}, the consumption of Mg^{2+} and carbonate by the dolomite-for-calcite replacement expressed by equation (4), its effect on pH, and the increasing reduction of aqueous sulfate by the organic matter released from the limestone by the replacement itself. The varying aqueous speciation during each pulse could help determine (1) what minimum Mg concentration the dolomitizing brine should contain for the rheological transition from replacive to displacive dolomite to be reached; (2) whether aqueous carbonate could become a limiting factor in the formation of dolomite during each pulse even before Mg^{2+} does, since the original brine is carbonate-poor and the replacement mass balance (equation 4) consumes carbonate; (3) how early or late within the course of a pulse will the release of organic matter from the limestone start, as well as the reduction of brine sulfate to sulfide by it, and the growth of Zn and Pb sulfides.

(4) An interesting possibility for future quantitative reaction-transport models of dolomitization based on the dynamics presented here will be to try to calculate the amount of ore precipitation per pulse and the degree of ore "sweeping" needed to form a large deposit downflow.

Finally, (5) there is the matter of modeling replacement itself as part of the reaction-transport modeling of dolomitization or any other process where replacements are known to take place. Since during any replacement the volumetric rates of guest growth and host dissolution are forced by the crystallization stress to be equal to each other at every moment (see Section III and fig. 3), reaction-transport modeling of a replacement should ensure that equality—an equality that the standard kinetic laws for guest and host would be unable to bring about by themselves if replacement is viewed as resulting by dissolution-precipitation. In modeling by reaction-transport the replacement of limestone by kaolinite that brings about the formation of *terra rossa,* Banerjee and Merino (2011) used rate laws from Fletcher and Merino (2001) to implement the desired rate equality. In the case of dolomitization, the equality of rates should take place even as they grow exponentially by the self-accelerating feedback.

Predicted periodic dissolution porosity.—Another interesting aim of future quantitative reaction-transport models might be to calculate the amount and perhaps spatial distribution of dissolution porosity. As noted, a basic feature of the dynamic model is that the considerable dissolution porosity carried out by the calcite-undersaturated dolomitizing brine when the brine enters the current limestone slice tends to be concentrated, for each pulse, at the entry into the slice (Section IV-11), and therefore would tend to be accumulated in the entry region of each slice. The predicted dissolution porosity should therefore be periodically distributed in space with a period roughly equal to L, the thickness of the slices, as shown schematically in figure 6. The predicted periodic porosity is confirmed by the interesting data presented by Budd and others (2006), but only in part, since they tease from their data *several* porosity periodicities, not just one. Therefore, future quantitative models could aim at improving the calculation of L that we present in table A1, Appendix 2. This would necessitate reliable estimates for the specific surface area and high-temperature growth rate constant of dolomite, and for the brine velocity through the limestone.

VI. SUMMARY OF THE MODEL

We propose a new dynamic model of burial dolomitization which is based on two postulates. The first is that the dolomitizing solution must be Mg-rich but *undersaturated* with respect to both dolomite and calcite. The second is that the replacement of limestone by dolomite takes place not by dissolution-precipitation as usually assumed, but by dolomite-growth-driven pressure solution of the calcite host.

The postulated brine dissolves some calcite as soon as it enters a limestone, generating dissolution porosity in the entry region and—only then—supersaturating itself with dolomite. Dolomite then grows as the brine infiltrates the limestone, pressure-dissolving, and thus replacing, more calcite. But the dolomite-for-calcite replacement turns out to be self-accelerating, via Ca^{2+}: the Ca^{2+} released by each increment of replacement must increase the ion-activity product for dolomite and thus rate of the next replacement increment, which increases Ca^{2+} further, and so on. As a result both the Ca^{2+} pore fluid concentration and the dolomite-for-calcite replacement rate increase exponentially with time, as the brine infiltrates the limestone.

The combination of chemical water/rock disequilibrium and positive feedback brings about temporally self-organized dynamics whereby the self-accelerating replacement takes place in repeated growth-and-replacement pulses, each of which shuts itself down when it becomes so fast that all available aqueous Mg is scavenged abruptly.

Towards the end of each pulse, as the pore fluid gets to contain a huge concentration of Ca^{2+}, calcite and other Ca-minerals such as fluorite and anhydrite, are also predicted to crystallize. In addition, if the dolomitizing brine contains Zn, Pb, Fe, Ba, F, sulfate, and other appropriate elements (as do brines from the Smackover Formation in Arkansas and the Central Mississippi Salt Dome basin, which seem to satisfy the first postulate of the model too), Mississippi-Valley-type (MVT) minerals will also precipitate at the end of each pulse. The replacement pulses repeat themselves automatically—each triggered by calcite dissolution by a new packet of brine—until the current slice of limestone under dolomitization is completely replaced. The thickness of the slice is determined by the velocity of brine infiltration and the time it takes for each pulse of replacement to become so fast that it shuts itself off abruptly. The dolomitization front thus remains fixed in space until the slice is completely replaced; only then does it jump to the next. Dolomite formed in late pulses may partly replace ore minerals formed in earlier pulses, partly "sweeping" the ores downflow. For a brine with 10^4 mg/ℓ of Mg infiltrating a 0.2 porosity limestone at 10 cm/year, each replacement pulse is calculated (table A1) to take place in <100 years, and about 200 pulses take place one after another until a limestone slice 0.5 to 5 meters thick is wholly replaced, in <20,000 years. (These calculations in table A1 were carried out for two values of the high-temperature rate constant for dolomite adopted loosely from Gautelier and others, 1999.)

Self-organization in pulses and slices thus accounts for: the generation of dissolution porosity, and its periodic distribution of maxima; the *complete* replacement of each limestone slice by dolomite, developing a sharp field contact between dolostone and unreplaced limestone; formation of late-stage calcite and MVT ores in each pulse; "sweeping" of ores downflow with ore accumulation in the last position of the dolomitization front; formation of fingers of dolomitization *via* the reactive infiltration instability.

In addition, for each pulse, the combination of the self-accelerating feedback via Ca^{2+} with the known strain-rate-softening, non-newtonian rheology of crystalline carbonates leads inevitably to an unlikely suite of associated textural, paragenetic, and geochemical predictions that are however strikingly confirmed by observation. If toward the end of a pulse the dolomite-for-calcite replacement rate gets to be fast enough to lower the viscosity of the local carbonate rock sufficiently (this needs a threshold concentration of Mg in the brine), then the dolomite growth, which has been replacive until that moment, is predicted to transition *seamlessly* to displacive. This is when displacive, self-organized zebra veins should form, making themselves equidistant by a secondary, "weeding" feedback described previously (Merino and others, 2006). Simultaneously with the fast dolomite growth near the end of each pulse, and regardless of whether the rheological transition has been reached, the Ca^{2+} pore fluid concentration becomes also so high that it drives substitution of Ca^{2+} for Mg^{2+}, or of submicroscopic calcitic slivers, on the structure of the growing dolomite crystals, replacive or displacive, forcing them to grow curved because of the larger size of Ca^{2+}. Also, the calcite may grow in interstices of the dolostone, and/or may replace some dolomite, a replacement known as dedolomitization. The predicted association of: *displacive, equidistant, thin* dolomitic veins displaying *seamless* contacts with their *replacive* walls; dolomite crystals that are *extra-calcic, curved,* and slightly *lower* in $\delta^{18}O$; and minor amounts of "late-stage" calcite, "dedolomite," and other Ca-bearing minerals (fluorite, anhydrite) and other MVT ores (galena, sphalerite) agrees very well with observations, and suggests that the new model captures the basic mechanisms, drives, and interactions that lend burial dolomitization and its often associated MVT mineralization its geological uniqueness.

ACKNOWLEDGMENTS

We thank our colleagues and guides to burial dolomites in Spain (Luis Villa, Fidel Grandía, Esteve Cardellach, Fernando Tornos, Gabriel Gutiérrez, Juan García Portero and Rafael Fenoy), Sardinia (Maria Boni, Naples) and Tunisia (Salah Bouhlel, Tunis). Thanks also to Raymond C. Murray for permission to reproduce his 1960 photomicrograph (see fig. 1A), the original of which was provided by W. H. Freeman & Co., publisher of H. Blatt, R. J. Tracy and B. E. Owens' *Petrology,* where we first saw it. To Marta Gasparrini of the Institut Français du Pétrole for permission to reproduce the photograph in figure 2A. To Greg Anderson, Toronto, for conversations on thermal sulfate reduction and for the hand sample of zebra veins from the Zn deposit at San Vicente, Peru (figs. 7C-D). To Richard J. Reeder, State University of New York at Stony Brook for conversations on the microstructures of saddle dolomites. To John Verhoogen, deceased, who inspired us to view geochemical processes dynamically. To Richard L. Hay, deceased, who brought home to us that replacement lies at the intersection of petrography and physical chemistry. To our friends Yifeng Wang of Sandia Labs, Carlos Ayora of the Spanish Council for Scientific Research at Barcelona, and Abhijit Basu of Indiana University for comments to previous drafts. And to Greg Anderson and an anonymous reviewer for their critical reviews of the manuscript for this Journal. Aspects of the new model were presented at the 2006 Goldschmidt Conference in Melbourne, the 2008 Gordon Conference on Ore Deposits at Barga, Italy, the 2010 annual meeting of the Sociedad Española de Mineralogía in Madrid, and the 2010 11th Conference on Mathematical Geophysics at Pisa.

Appendix 1

Dolomite Growth Rate and Ca^{2+} Concentration in Pore Fluid Increase Exponentially With Time

By equations (5, 5a) the growth rate of dolomite is

$$R_{dolomite} \approx k_{dolo} S_0 (\Omega - 1), \tag{5a}$$

where

$$\Omega = Q/K_{eq}^{dolo} = (m_{Ca2+}\gamma_{Ca2+})(a_{Mg2+})(a_{CO3})^2/K_{eq}^{dolo}, \tag{5}$$

where the equilibrium constant is consistent with molality units but dimensionless, the activities of Mg^{2+} and CO_3^{2-} are also dimensionless and the activity of Ca^{2+} is written as (molarity of Ca^{2+} in moles/ℓ) $\times$ (Ca^{2+} activity coefficient, in ℓ/mole) assuming for simplicity that molality is approximately equal to molarity. The quantities ($k_{dolo}S_0$) and $R_{dolomite}$ have units of moles/ℓ second. Since the Mg^{2+} and CO_3^{2-} activities remain roughly constant during, say, the first two-thirds of each pulse of replacement (see eqs 5, 5a and text, and fig. 5B), and since the supersaturation Ω becomes $\gg$1, the "-1" can be neglected in (5a):

$$R_{dolo} \approx k_{dolo} S_0 \{(a_{Mg2+})(a_{CO3})^2/K_{eq}^{dolo}\}(m_{Ca2+}\gamma_{Ca2+}). \tag{A1}$$

Note that the local mass conservation equation for Ca^{2+} probably involves little or no transport because, as the incipient dolomite growth is starting to replace calcite everywhere, both the Ca^{2+} and Mg^{2+} profiles remain horizontal and preclude diffusion of Ca^{2+} or Mg^{2+} forward or backwards. Thus,

$$\mathrm{d}\, m_{Ca2+}/\mathrm{d}t = hR_{dolo}, \tag{A2}$$

where h is the stoichiometric coefficient of Ca^{2+} in the replacement mass balance (4), 0.74 moles of Ca^{2+} released to pore fluid/dolomite formula, and molality m is again expressed in molarity units. Putting (A1) into (A2), and moving m_{Ca2+} to the left side and dt to the right, one obtains

$$\begin{aligned} \mathrm{d}\, m_{Ca2+}/m_{Ca2+} &= hk_{dolo}S_0\{(\gamma_{Ca2+})(a_{Mg2+})(a_{CO3})^2/K_{eq}^{dolo}\}\mathrm{d}t \\ &= hk_{dolo}S_0 H\mathrm{d}t \end{aligned} \tag{A3}$$

where

$$H = (\gamma_{Ca2+})(a_{Mg2+})(a_{CO3})^2/K_{eq}^{dolo}. \tag{A4}$$

TABLE A1

*Calculated values of T, L, and N for two dolomite growth rate constants, 10^{-14} (left table) & 10^{-15} mol/cm^2 s (right table),** for a brine with 10^4 mg of Mg/ℓ infiltrating limestone at 10 cm/year*

Parameters Used		Parameters Used	
$k_{dolo,100C}$	10^{-14} mol/cm^2 s	$k_{dolo,100C}$	10^{-15} mol/cm^2 s
h	0.75 mol(Ca)/mol(do)	h	0.75 mol(Ca)/mol(do)
b	64 cm^3(do)/mol Mg	b	64 cm^3(do)/mol Mg
S_0	100 cm^2/cm^3	S_0	100 cm^2/cm^3
ρ(dolo)	0.0156 mol/cm^3	ρ(dolo)	0.0156 mol/cm^3
poro, ϕ	0.2	poro, ϕ	0.2
veloc, v	10 cm/yr	veloc, v	10 cm/yr
$m(Mg)_{initial}$	0.4 mol/ℓ = 10^4 mg/ℓ	$m(Mg)_{initial}$	0.4 mol/ℓ = 10^4 mg/ℓ
$m(Ca)_{initial}$	1.00 mol/ℓ	$m(Ca)_{initial}$	1.00 mol/ℓ
γ(Ca, Mg)	0.3 ℓ/mol	γ(Ca, Mg)	0.3 ℓ/mol
activ(CO3)	3.16E-09	activ(CO3)	3.16E-09
activ(Mg)	1.20E-01	activ(Mg)	1.20E-01
K_{eq}(do), 100°C	6.76E-21*	K_{eq}(do), 100°C	6.76E-21*
Calculated Quantities		Calculated Quantities	
H (eq A4)	5.32E+01 ℓ/mol	H (eq A4)	5.32E+01 ℓ/mol
τ (eq A6)	2.50E+07 s = 0.8 yrs	τ (eq A6)	2.50E+08 s = 8 yrs
T (eq A7)	1.73E+08 s = 5.5 yrs	T (eq A7)	1.73E+09 s = 55 yrs
L = vT	55 cm	L = vT	5.5 m
R(dolo), eq A7	5.32E-08 mol/cm^3 s	R(dolo), eqA7	5.32E-09 mol/cm^3 sec
R'(dolo)	0.088 cm/month	R'(dolo)	0.009 cm/month
$N=1/\phi c_{Mg} b$	195 pulses	$N=1/\phi c_{Mg} b$	195 pulses

* Bowers and others (1984).

**Rate-constant values were loosely extrapolated from values graphed by Gautelier and others, 1999. T is the time it takes for the replacement rate R to become 1000 times greater than it was at the start of each growth pulse, by which time aqueous Mg is used up abruptly; L is the thickness of limestone slice affected by each pulse in the time T; N is the number of pulses needed to replace each slice of thickness L completely.

By integration of (A3) from $m_{Ca2+,initial}$ to m_{Ca2+} and from $t = 0$ to $t = t$, one gets

$$m_{Ca2+} = m_{Ca2+,initial} \exp(t/\tau), \tag{A5}$$

where

$$\tau = (1000 h k_{dolo} S_0 H)^{-1} \tag{A6}$$

has units of time and the 1000 factor converts liters in the H units to cm^3 in the $(k_{dolo}S_0)$ units. From (A1, A5),

$$R_{dolo} \approx (k_{dolo} S_0 H m_{Ca2+,initial}) \exp(t/\tau). \tag{A7}$$

In short, because of the feedback between the two, *both* the pore-fluid Ca^{2+} concentration and dolomite growth rate increase exponentially with time, eqs (A5, A7), as shown in figure 5A.

APPENDIX 2

Replacement of One Limestone Slice By Many Pulses

With reference to figure 6, replacement of a limestone slice takes place *completely* by many sequential pulses of dolomite growth (plus minor calcite and ores). Each pulse of dolomite precipitation grows—at a self-accelerating rate—from the Mg-rich pore brine contained in the slice's pores, lasts a time T calculated in Appendix 1, and has an approximate length $L = vT$. T is the time it takes for the dolomitization to become so fast that all the aqueous Mg in the slice is used up instantaneously. "v" is the velocity of brine through the limestone pores. Each pulse can replace only a fraction $f = (\phi v c_{Mg}) TAb/vTA = \phi c_{Mg} b$ of the limestone slice's volume. Successive batches of brine keep filling the pores of the current slice and keep precipitating pulses of dolomite, each pulse using up *abruptly* all the aqueous Mg^{2+} in the slice after a time T. N $(=1/\phi c_{Mg} b)$ pulses are necessary to replace the slice completely.

For the following values of Mg concentration in the initial brine and rock porosity

$$c_{Mg} = 10{,}000 \text{ mg}/\ell = (10/24) \times 10^{-3} \text{ mol Mg/cm}^3 \text{ pore} = 0.4 \times 10^{-3} \text{ mol Mg/cm}^3;$$

$$\phi = 0.2 \text{ cc pore/cc bulk rock;}$$

and

$$b = 64 \text{ cm}^3 \text{ of dolo/mol Mg}^{2+},$$

a fraction $f = 0.2 \times (0.4 \times 10^{-3}$ mol Mg/cm^3 pore$) \times (64$ cm^3 dolo/mol Mg$) \approx 0.005 = 0.5$ percent is dolomitized by one pulse (in time T), and $N = 1/f \approx 200$ fillings, lasting roughly a time $200T$, are needed to completely dolomitize that one slice, or reaction zone, of limestone. With parameter values adopted in table A1 and equations A4, A6 we calculate estimates of H, τ, and the time T needed for R(dolo) to become 1000 times greater than it was at t = 0+. The value of the dolomite growth rate at $t = T$ is given in mole/cm^3 s as R(dolo) and in cm/month as R'(dolo). All the calculations are performed for two estimates, 10^{-14} and 10^{-15} mol/cm^2 s, of the high-temperature dolomite-growth rate constant in equation 5a. The dolomite rate-constant values chosen were loosely extrapolated from rates graphed vs *p*H by Gautelier and others (1999, their fig. 7). The time T for one growth pulse is 5.5 and 55 years, respectively, yielding, for an arbitrary brine velocity of 10 cm/year, a slice thickness, or thickness of the reaction zone, of 55 cm and 5.5 meters, respectively.

Since dolomitization of limestone self-accelerates exponentially on time, brine with concentration c_{Mg} (mol Mg/cm^3 of pore fluid) infiltrates limestone of porosity ϕ over a thickness vT, where T is the time it takes for the dolomitization to become so fast that all the aqueous Mg in the segment is used up instantaneously, and v is the brine velocity through the limestone pores. That length, vT, is the thickness L of the reaction zone. The reaction zone remains stationary until all the limestone in it is completely dolomitized. Each successive packet of Mg brine that fills the pores of the reaction zone drops a pulse of dolomite which replaces only a fraction f of the current limestone slice. $N = 1/f$ "fillings" are needed to dolomitize the slice completely.

The volume of dolomite made by one "filling" of the limestone volume vTA with brine is:

$$V_{dolo,T} = (\text{flux}) \times (\text{time } T) \times (\text{cross section A}) \times (b) = (\phi v c_{Mg}) TAb, \tag{B1}$$

where $b = 64$ cm^3 dolo/mol Mg^{2+}.

The initial bulk volume of limestone containing V_{doloT} is:

$$V_{limest} = vTA. \tag{B2}$$

Thus the volume fraction dolomitized in each pulse is:

$$f = (\phi v c_{Mg}) TAb / vTA = \phi c_{Mg} b. \tag{B3}$$

(Note that this is independent of T, the duration of one pulse, which can be calculated from Appendix 1. Once T is known we can calculate the length of one "pulse," or thickness of the "reaction zone," equal to vT.) The number of fillings needed to dolomitize one reaction zone completely is

$$N = 1/\phi c_{Mg} b. \tag{B4}$$

References

Adams, A. E., MacKenzie, W. S., and Guilford, C., 1984, Atlas of Sedimentary Rocks under the Microscope: New York, Longman and John Wiley & Sons, p. 104.

Aharonov, E., Spiegelman, M., and Kelemen, P., 1997, Three-dimensional flow and reaction in porous media: Implications for the Earth's mantle and sedimentary basins: Journal of Geophysical Research, v. 102, n. B7, p. 14,821–14,834, http://dx.doi.org/10.1029/97JB00996

Anderson, G. M., and Thom, J., 2008, The role of thermochemical sulfate reduction in the origin of Mississippi Valley-type deposits. II. Carbonate-sulfide relationships: Geofluids, v. 8, p. 27–34, http://dx.doi.org/10.1111/j.1468-8123.2007.00202.x

Banerjee, A., and Merino, E., 2011, Terra Rossa genesis by replacement of limestone by Kaolinite: III. Dynamic quantitative model: The Journal of Geology v. 119, n. 3, p. 259–274, http://dx.doi.org/10.1086/659146

Barber, D. J., Reeder, R. J., and Smith, D. J., 1985, A tem microstructural study of dolomite with curved faces (saddle dolomite): Contributions to Mineralogy and Petrology, v. 91, n. 1, p. 82–92, http://dx.doi.org/10.1007/BF00429430

Bastin, E. S., 1950, Interpretation of Ore Textures: Geological Society of America Memoir, v. 45, 101 p.

Bastin, E. S., Graton, L. C., Lindgren, W., Newhouse, W. H., Schwartz, G. M., and Short, M. N., 1931, Criteria

of age relations of minerals, with especial reference to polished sections of ores: Economic Geology, v. 26, n. 6, p. 561–610, http://dx.doi.org/10.2113/gsecongeo.26.6.561
Benito, M. I., Lohmann, K. C., and Mas, R., 2006, Micro-sized dolomite inclusions in ferroan calcite cements developed during burial diagenesis of Kimmeridgian reefs, Northern Iberian Basin, Spain: Journal of Sedimentary Research, v. 76, n. 3, p. 472–482, http://dx.doi.org/10.2110/jsr.2006.042
Bethke, C. M., and Marshak, S., 1990, Brine migrations across North America—The plate tectonics of groundwater: Annual Reviews of Earth and Planetary Sciences, v. 18, p. 287–315, http://dx.doi.org/10.1146/annurev.ea.18.050190.001443
Bons, P. D., 2000, The formation of veins and their microstructures, *in* Jessell, M. W., and Urai, J. L., editors, Stress, Strain, and Structure, A Volume in Honor of W. D. Means: Journal of the Virtual Explorer, v. 2.
Bowers, T. S., Jackson, K. J., and Helgeson, H. C., 1984, Equilibrium Activity Diagrams: Berlin, Springer-Verlag, 397 p.
Budd, D. A., Pranter, M. J., and Rezza, Z. A., 2006, Lateral periodic variations in the petrophysical and geochemical properties of dolomite: Geology, v. 34, n. 5, p. 373–376, http://dx.doi.org/10.1130/G22132.1
Carmichael, D. M., 1987, Induced stress and secondary mass transfer: Thermodynamic basis for the tendency toward constant-volume constraint in diffusion metasomatism, *in* Helgeson, H. C., editor, Chemical Transport in Metasomatic Processes: NATO Advanced Study Institute Series C, v. 218, p. 239–264.
Carmichael, S. K., Ferry, J. M., and McDonough, W. F., 2008, Formation of replacement dolomite in the Latemar Carbonate Buildup, Dolomites, Northern Italy: Part 1. Field relations, mineralogy, and geochemistry: American Journal of Science, v. 308, p. 851–884, http://dx.doi.org/10.2475/07.2008.03
Caspard, E., Rudkiewicz, J. L., Eberli, G. P., Brosse, E., and Renard, M., 2004, Massive dolomitization of a Messinian reef in the Great Bahama Bank: a numerical modelling evaluation of Kohout geothermal convection: Geofluids, v. 4, n. 1, p. 40–60, http://dx.doi.org/10.1111/j.1468-8123.2004.00071.x
Chadam, J., Hoff, D., Merino, E., Ortoleva, P., and Sen, A., 1986, Reactive infiltration instability: IMA Journal of Applied Mathematics, v. 36, n. 3, p. 207–221, http://dx.doi.org/10.1093/imamat/36.3.207
Chen, D., Quing, H., and Yang, Ch., 2004, Multistage hydrothermal dolomites in the Middle Devonian (Givetian) carbonates from the Guilin area, South China: Sedimentology, v. 51, n. 5, p. 1029–1051, http://dx.doi.org/10.1111/j.1365-3091.2004.00659.x
Choquette, P. W., and Hiatt, E. E., 2008, Shallow-burial dolomite cement: a major component of many ancient sucrosic dolomites: Sedimentology, v. 55, n. 2, p. 423–460, http://dx.doi.org/10.1111/j.1365-3091.2007.00908.x
Corbella, M., Ayora, C., and Cardellach, E., 2004, Hydrothermal mixing, carbonate dissolution and sulphide precipitation in Mississippi-Valley type deposits: Mineralium Deposita, v. 39, n. 3, p. 344–357, http://dx.doi.org/10.1007/s00126-004-0412-5
Davies, G. R., and Smith, L. B., Jr., 2006, Structurally controlled hydrothermal dolomite reservoir facies: An overview: AAPG (American Association of Petroleum Geologists) Bulletin, v. 90, p. 1641–1690, http://dx.doi.org/10.1306/05220605164
Dewers, T., and Ortoleva, P., 1989, Mechano-chemical coupling in stressed rocks: Geochimica et Cosmochimica Acta, v. 53, p. 1243–1258, http://dx.doi.org/10.1016/0016-7037(89)90060-4
Fletcher, R. C., and Merino, E., 2001, Mineral growth in solid rock: kinetics and rheology in replacement, vein formation, and tectonic crystallization: Geochimica et Cosmochimica Acta, v. 65, n. 21, p. 3733–3748, http://dx.doi.org/10.1016/S0016-7037(01)00726-8
Fontboté, L., 1993, Self-organization fabrics in carbonate-hosted ore deposits: Example of diagenetic crystallization rhythmites, *in* Fenoll Hach-Alí, P., Torres-Ruiz, J., and Gervilla, F., editors, Current Research in Geology Applied to Ore Deposits: Granada, University of Granada, p. 11–14.
Fontboté, L., and Amstutz, G. C., 1980, New observations on diagenetic crystallization rhythmites in the carbonate facies of the Triassic of the Alpujárrides (Betic Cordillera, Spain): Comparison with other diagenetic rhythmites: Revista del Instituto de Investigaciones Geológicas, v. 34, p. 293–310.
Fontboté, L., and Gorzawski, H., 1990, Genesis of the Mississippi Valley-type Zn-Pb deposit of San Vicente, Central Peru: Geologic and isotopic (Sr, O, C, S, Pb) evidence: Economic Geology, v. 85, p. 1402–1437, http://dx.doi.org/10.2113/gsecongeo.85.7.1402
Garrels, R. M., 1960, Mineral Equilibria: New York, Harper and Brothers, 254 p.
Garrels, R. M., and Christ, C. L., 1965, Solutions, Minerals and Equilibria: New York, Harper and Row, 450 p.
Garven, G., Ge, S., Person, M. A., and Sverjensky, D. A., 1993, Genesis of stratabound ore deposits in the midcontinent basins of North America. 1. The role of regional groundwater flow: American Journal of Science, v. 293, p. 497–568. http://dx.doi.org/10.2475/ajs.293.6.497
Gasparrini, M., ms, 2003, Large-scale hydrothermal dolomitisation in the southwestern Cantabrian Zone (NW Spain): Causes and controls of the process and origin of the dolomitising fluids: Heidelberg, Germany, University of Heidelberg, Ph.D. thesis, 203 p.
Gasparrini, M., Bechstädt, T., and Boni, M., 2006, Massive hydrothermal dolomites in the southwestern Cantabrian Zone (Spain) and their relation to the Late Variscan Evolution: Marine and Petroleum Geology, v. 23, p. 543–568, http://dx.doi.org/10.1016/j.marpetgeo.2006.05.003
Gautelier, M., Oelkers, E. H., and Schott, J., 1999, An experimental study of dolomite dissolution rates as a function of pH from −0.5 to 5 and temperature from 25 to 80°C: Chemical Geology, v. 157, n. 1–2, p. 13–26. http://dx.doi.org/10.1016/S0009-2541(98)00193-4
Gregg, J. M., 2004, Basin fluid flow, base-metal sulphide mineralization and the development of dolomite petroleum reservoirs, *in* Braithwaite, C. J. R., Rizzi, G., and Darke, G., editors, The geometry and petrogenesis of dolomite hydrocarbon reservoirs: Geological Society, London, Special Publications, v. 235, p. 157–175. http://dx.doi.org/10.1144/GSL.SP.2004.235.01.07
Gregg, J. M., Shelton, K. L., Johnson, A. W., Somerville, I. D., and Wright, W. R., 2001, Dolomitization of the

Waulsortian Limestone (Lower Carboniferous) Irish Midlands: Sedimentology, v. 48, n. 4, p. 745–766, http://dx.doi.org/10.1046/j.1365-3091.2001.00397.x
Harker, A., 1950, Metamorphism: 3rd edition: London, Methuen, 362 p.
Harper, D. D., and Borrok, D. M., 2007, Dolomite fronts and associated zinc-lead mineralization, USA: Economic Geology, v. 102, n. 7, p. 1345–1352. http://dx.doi.org/10.2113/gsecongeo.102.7.1345
Heard, H. C., and Raleigh, C. B., 1972, Steady-state flow in marble at 500 to 800 °C: Geological Society of America Bulletin, v. 83, n. 4, p. 935–956, http://dx.doi.org/10.1130/0016-7606(1972)83[935:SFIMAT]2.0.CO;2
Helgeson, H. C., 1968, Evaluation of irreversible reactions in geochemical processes involving minerals and aqueous solutions—I. Thermodynamic relations: Geochimica et Cosmochimica Acta, v. 32, p. 853–877, http://dx.doi.org/10.1016/0016-7037(68)90100-2
Helgeson, H. C., Garrels, R. M., and Mackenzie, F. T., 1969, Evaluation of irreversible reactions in geochemical processes involving minerals and aqueous solutions—II. Applications: Geochimica et Cosmochimica Acta, v. 33, n. 4, p. 455–481, http://dx.doi.org/10.1016/0016-7037(69)90127-6
Hitzman, M. W., Allan, J. R., and Beaty, D. W., 1998, Regional dolomitization of the Waulsortian limestone in southeastern Ireland: evidence of large-scale fluid flow driven by the Hercynian orogeny: Geology, v. 26, n. 6, p. 547–550, http://dx.doi.org/10.1130/0091-7613(1998)126⟨0547:RDOTWL⟩2.3.CO;2
Horton, R. A., 1989, Origin of zebra texture in dolomite: Evidence from the Leadville Dolomite (Mississippian), Central Colorado: Geological Society of America Abstracts with Programs, v. 21, n. 5, p. 97.
Jones, G. D., and Xiao, Y., 2005, Dolomitization, anhydrite cementation, and porosity evolution in a reflux system: Insights from reactive transport models: AAPG (American Association of Petroleum Geologists) Bulletin, v. 89, n. 5, p. 577–601, http://dx.doi.org/10.1306/12010404078
Kharaka, Y. K., Maest, A. S., Carothers, W. W., Law, L. M., Lamothe, P. J., and Fries, T. L., 1987, Geochemistry of metal-rich brines from central Mississippi Salt Dome basin, U.S.A.: Applied Geochemistry, v. 2, p. 543–561, http://dx.doi.org/10.1016/0883-2927(87)90008-4
Land, L. S., 1980, The isotopic and trace-element geochemistry of dolomite: The state of the art, *in* Zenger, D., Dunham, J. B., and Ethington, R. L., editors, Concepts and models of dolomitization: SEPM (Society for Economic Palaeontologists and Mineralogists) Special Publication, v. 28, p. 87–110. http://dx.doi.org/10.2110/pec.80.28.0087
Lindgren, W., 1912, The nature of replacement: Economic Geology, v. 7, n. 6, p. 521–535, http://dx.doi.org/10.2113/gsecongeo.7.6.521
——— 1925, Metasomatism: Geological Society of America Bulletin, v. 36, n. 1, p. 247–261.
Lonnee, J., and Machel, H. G., 2006, Pervasive dolomitization with subsequent hydrothermal alteration in the Clarke Lake gas field, Middle Devonian Slave Point Formation, British Columbia, Canada: American Association of Petroleum Geologists (AAPG) Bulletin, v. 90, p. 1739–1761, http://dx.doi.org/10.1306/03060605069
Machel, H. G., 2004, Concepts and models of dolomitization: a critical reappraisal, *in* Braithwaite, C. J. R., Rizzi, G., and Darke, G., editors, The geometry and petrogenesis of dolomite hydrocarbon reservoirs: Geological Society, London, Special Publications, v. 235, p. 7–63, http://dx.doi.org/10.1144/GSL.SP.2004.235.01.02
Maliva, R. G., and Siever, R., 1988, Diagenetic replacement controlled by force of crystallization: Geology, v. 16, n. 8, p. 688–691, http://dx.doi.org/10.1130/0091-7613(1988)016⟨0688:DRCBFO⟩2.3.CO;2
Mattes, B. W., and Mountjoy, E. W., 1980, Burial dolomitization of the Upper Devonian Miette Buildup, Jasper National Park, Alberta, *in* Zenger, D. H., Dunham, J. B., and Ethington, R. L., editors, Concepts and Models of Dolomitization: SEPM (Society for Economic Palaeontologists and Mineralogists) Special Publication, v. 28, p. 259–297. http://dx.doi.org/10.2110/pec.80.28.0259
McLimans, R. K., Barnes, H. L., and Ohmoto, H., 1980, Sphalerite stratigraphy of the Upper Mississippi Valley zinc-lead district, Southwest Wisconsin: Economic Geology, v. 75, p. 351–361, http://dx.doi.org/10.2113/gsecongeo.75.3.351
Merino, E., 1979, Internal consistency of a water analysis and uncertainty of the calculated distribution of species at 25°C: Geochimica et Cosmochimica Acta, v. 43, n. 9, p. 1533–1542, http://dx.doi.org/10.1016/0016-7037(79)90146-7
——— 1984, Survey of geochemical self-patterning phenomena, *in* Nicolis, G., and Baras, F., editors, Chemical Instabilities: Applications in Chemistry, Engineering, Geology, and Materials Science: D. Reidel Publishing, NATO Advanced Science Series C, v. 120, p. 305–328.
Merino, E., and Banerjee, A., 2008, Terra rossa genesis, implications for karst, and eolian dust: A geodynamic thread: Journal of Geology, v. 116, n. 1, p. 62–75, http://dx.doi.org/10.1086/524675
Merino, E., and Dewers, T., 1998, Implications of replacement for reaction-transport modeling: Journal of Hydrology, v. 209, p. 137–146, http://dx.doi.org/10.1016/S0022-1694(98)00150-4
Merino, E., and Wang, Y., 2001, Self-organization in rocks: Occurrences, observations, modeling, testing—with emphasis on agate genesis, *in* Krug, H.-J., and Kruhl, J. H., editors, Nichtgleichgewichtsprozesse und dissipative Strukturen in den Geowissenschaften (Non-equilibrium processes and dissipative structures in the earth sciences): Selbstorganisation. Jahrbuch für Komplexität in den Natur-, Sozial- und Geisteswissenschaften. (Self-organization. Yearbook of complexity in the natural sciences, social sciences and humanities), v. 11(2000), p. 13–35: Berlin, Dunker, and Humblot, 380 p.
Merino, E., Nahon, D., and Wang, Y., 1993, Kinetics and mass transfer of replacement: application to replacement of parent minerals and kaolinite by Al, Fe and Mn oxides during weathering: American Journal Science, v. 293, p. 135–155, http://dx.doi.org/10.2475/ajs.293.2.135
Merino, E., Canals, A., and Fletcher, R. C., 2006, Genesis of self-organized zebra textures in burial dolomites: Displacive veins, induced stress, and dolomitization: Geologica Acta, v. 4, n. 3, p. 383–393, http://dx.doi.org/10.1344/105.000000352
Moldovanyi, E. P., and Walters, L. M., 1992, Regional trends in water chemistry, Smackover Formation,

southwest Arkansas: Geochemical and physical controls: AAPG (American Association of Petroleum Geologists) Bulletin, v. 76, p. 864–894.
Montañez, I. P., and Read, J. F., 1992, Fluid-rock interaction history during the stabilization of early dolomites, Upper Knox Group (Lower Ordovician), U.S. Appalachians: Journal of Sedimentary Petrology, v. 62, p. 753–778, http://dx.doi.org/10.1306/D42679D3-2B26-11D7-8648000102C1865D
Nahon, D., and Merino, E., 1997, Pseudomorphic replacement in tropical weathering: Evidence, geochemical consequences, and kinetic-rheological origin: American Journal of Science, v. 297, p. 393–417, http://dx.doi.org/10.2475/ajs.297.4.393
Nielsen, P., Swennen, R., Muchez, P. H., and Keppens, E., 1998, Origin of Dinantian zebra dolomites south of the Brabant-Wales Massif, Belgium: Sedimentology, v. 45, n. 4, p. 727–743, http://dx.doi.org/10.1046/j.1365-3091.1998.00171.x
O'Neil, J. R., 1986, Theoretical and experimental aspects of isotopic fractionation, *in* Valley, J. V., Taylor, H. P., Jr., and O'Neil, J. R., editors. Stable Isotopes and High-Temperature Geological Processes: Reviews in Mineralogy, v. 16, p. 1–40.
Ortoleva, P., Auchmuty, G., Chadam, J., Hettmer, J., Merino, E., Moore, C. H., and Ripley, E., 1986, Redox front propagation and banding modalities: Physica D, v. 19, n. 3, p. 334–354, http://dx.doi.org/10.1016/0167-2789(86)90063-1
Ortoleva, P., Merino, E., Moore, C., and Chadam, J., 1987a, Geochemical self-organization, I. Feedbacks and quantitative modeling: American Journal of Science v. 287, p. 979–1007, http://dx.doi.org/10.2475/ajs.287.10.979
Ortoleva, P., Chadam, J., Merino, E., and Sen, A., 1987b, Geochemical self-organization, II. The reactive-infiltration instability in water-rock systems: American Journal of Science, v. 287, p. 1008–1040, http://dx.doi.org/10.2475/ajs.287.10.1008
Pettijohn, F. J., 1957, Sedimentary Rocks: New York, Harper & Row, second edition, 718 p.
PHREEQC, version 2: A computer program for speciation, batch reaction, one-dimensional transport, and inverse geochemical calculations, http://wwwbrr.cr.usgs.gov/projects/GWC_coupled/phreeqc/
Plumlee, G. S., Goldhaber, M. B., and Rowan, E. L., 1995, The potential role of magmatic gases in the genesis of Illionois-Kentucky fluorspar deposits: Implications from chemical reaction path modeling: Economic Geology, v. 90, n. 5, p. 999–1011. http://dx.doi.org/10.2113/gsecongeo.90.5.999
Putnis, A., 2009, Mineral Replacement Reactions, *in* Oelkers, E. H., and Schott, J., editors, Thermodynamics and Kinetics of Water-Rock Interaction: Reviews in Mineralogy and Geochemistry, v. 70, p. 87–124, http://dx.doi.org/10.2138/rmg.2009.70.3
Radke, B. M., and Mathis, R. L., 1980, On the formation and occurrence of saddle dolomite: Journal of Sedimentary Petrology, v. 50, p. 1149–1168, http://dx.doi.org/10.1306/212F7B9E-2B24-11D7-8648000102C1865D
Robinson, R. A., and Stokes, R. H., 1959, Electrolyte Solutions, second edition, revised: London, Butterworths, 571 p.
Savard, M. M., Chi, G., Sami, T., Williams-Jones, A. E., and Leigh, K., 2000, Fluid inclusion and carbon, oxygen, and strontium isotope study of the Polaris Mississippi Valley-type Zn-Pb deposit, Canadian Arctic Archipelago: implications for ore genesis: Mineralium Deposita, v. 35, n. 6, p. 495–510, http://dx.doi.org/10.1007/s001260050257
Sibson, R. H., 1994, Crustal stress, faulting, and fluid flow, *in* Parnell, J., editor, Geofluids: Origin, Migration and Evolution of Fluids in Sedimentary Basins: Geological Society, London, Special Publications, v. 78, p. 69–84, http://dx.doi.org/10.1144/GSL.SP.1994.078.01.07
Simón, S., Canals, À., Grandía, F., and Cardellach, E., 1999, Estudio isotópico y de inclusiones fluidas en depósitos de calcita y dolomita del sector oeste del Anticlinal de Bilbao, y su relación con las mineralizaciones de Fe-Zn-Pb: Boletín de la Sociedad Española de Mineralogía, v. 22, p. 55–71.
Spirakis, C. S., and Heyl, A. V., 1995, Evaluation of proposed precipitation mechanism for Mississippi Valley-type deposits: Ore Geology Reviews, v. 10, p. 1–17, http://dx.doi.org/10.1016/0169-1368(95)00008-P
Sverjensky, D. A., 1981, The Origin of a Mississippi Valley-Type Deposit in the Viburnum Trend, Southeast Missouri: Economic Geology, v. 76, n. 7, p. 1848–1872, http://dx.doi.org/10.2113/gsecongeo.76.7.1848
Szymczak, P., and Ladd, A. J. C., 2006, A network model of cannel competition in fracture dissolution: Geophysical Research Letters, v. 33, L05401, 4 p., http://dx.doi.org/10.1029/2005GL025334
Thom, J., and Anderson, G. M., 2008, The role of thermochemical sulfate reduction in the origin of Mississippi Valley-type deposits I. Experimental results: Geofluids, v. 8, n. 1, p. 16–26, http://dx.doi.org/10.1111/j.1468-8123.2007.00201.x
Tona, F., ms, 1973, Positions des horizons dolomitiques minéralisés en fluorine et galène au sein des sédiments Triasiques de la Sierra de Lújar (Grenade): Évolution et géochimie: Paris, France, Université de Paris-VI, Ph. D. thesis, 166 p.
Vandeginste, V., Swennen, R., Gleeson, S. A., Ellam, R. M., Osadetz, K., and Roure, F., 2005, Zebra dolomitization as a result of focused fluid flow in the Rocky Mountains Fold and Thrust Belt, Canada: Sedimentology, v. 52, n. 5, p. 1067–1095, http://dx.doi.org/10.1111/j.1365-3091.2005.00724.x
Verhoogen, J., Turner, F. J., Weiss, L. E., Wahrhaftig, C., and Fyfe, W. S., 1970, The Earth: New York, Holt, Rinehart and Winston, 748 p.
Wallace, M. W., Both, R. A., Morales Ruano, S., Fenoll Hach-Ali, P., and Lees, T., 1994, Zebra textures from carbonate-hosted sulfide deposits: Sheet cavity networks produced by fracture and solution enlargement: Economic Geology, v. 89, n. 5, p. 1183–1191, http://dx.doi.org/10.2113/gsecongeo.89.5.1183
Wei, C., and Ortoleva, P., 1990, Reaction-front fingering in carbonate-cemented sandstones: Earth-Science Reviews, v. 29, n. 1–4, p. 183–198, http://dx.doi.org/doi:10.1016/0012-8252(0)90036-U
Weyl, P. K., 1959, Pressure solution and the force of crystallization—A phenomenological theory: Journal of Geophysical Research, v. 64, n. 11, p. 2001–2025, http://dx.doi.org/10.1029/JZ064i011p02001

——— 1960, Porosity through dolomitization: conservation-of-mass requirements: Journal of Sedimentary Petrology, v. 30, n. 1, p. 85–90, http://dx.doi.org/10.1306/74D709CF-2B21-11D7-8648000102C1865D

Whittaker, F. F., Smart, P. L., and Jones, G. D., 2004, Dolomitization: From conceptual to numerical models *in* Braithwaite, C. J. R., Rizzi, G., and Darke, G., editors, The Geometry and Petrogenesis of Dolomite Hydrocarbon Reservoirs: Geological Society, London, Special Publications, v. 235, p. 99–139, http://dx.doi.org/10.1144/GSL.SP.2004.235.01.05

Wilkinson, J. J., 2003, On diagenesis, dolomitisation and mineralisation in the Irish Zn-Pb orefield: Mineralium Deposita, v. 38, n. 8, p. 968–983, http://dx.doi.org/10.1007/s00126-003-0387-7

Wilson, A. M., Sanford, W., Whittaker, F. F., and Smart, P., 2001, Spatial patterns of diagenesis during geothermal circulation in carbonate platforms: American Journal of Science, v. 301, p. 727–752, http://dx.doi.org/10.2475/ajs.301.8.727

Wilson, E. N., Hardie, L. A., and Phillips, O. M., 1990, Dolomitization front geometry, fluid flow patterns, and the origin of massive dolomite: The Triassic Latemar buildup, northern Italy: American Journal of Science, v. 290, p. 741–796, http://dx.doi.org/10.2475/ajs.290.7.741

Wiltschko, D. V., and Morse, J. W., 2001, Crystallization pressure versus "crack seal" as the mechanism for banded veins: Geology, v. 29, n. 1, p. 79–82, http://dx.doi.org/10.1130/0091-7613(2001)029⟨0079:CPVCSA⟩2.0.CO;2

Yao, Q., and Demicco, R. V., 1997, Dolomitization of the Cambrian carbonate platform, Southern Canadian Rocky Mountains: Dolomite front geometry, fluid inclusion geochemistry, isotopic signature, and hydrogeologic modeling studies: American Journal of Science, v. 297, p. 892–938, http://dx.doi.org/10.2475/ajs.297.9.892

Zeeh, S., 1995, Complex replacement of saddle dolomite by fluorite within zebra dolomites: Mineralium Deposita, v. 30, n. 6, p. 469–475, http://dx.doi.org/10.1007/BF00196406

Zenger, D. H., and Dunham, J. B., 1980, Concepts and models of dolomitization—An introduction, *in* Zenger, D. H., Dunham, J. B., and Ethington, R. L., editors, Concepts and models of dolomitization: Society of Economic Paleontologists and Mineralogists, Special Publication, v. 28, p. 1–9.